UPPSALA UNIVERSITET

Digital Comprehensive Summaries of Uppsala Dissertations from the Faculty of Medicine 1456

Visualization of Peripheral Pain Generating Processes and Inflammation in Musculoskeletal Tissue using [^{11}C]-D-deprenyl PET

MIKKO AARNIO

ACTA
UNIVERSITATIS
UPSALIENSIS
UPPSALA
2018

ISSN 1651-6206
ISBN 978-91-513-0313-0
urn:nbn:se:uu:diva-347685

Dissertation presented at Uppsala University to be publicly examined in Universitetshuset, Biskopsgatan 3, Uppsala, Friday, 25 May 2018 at 09:00 for the degree of Doctor of Philosophy (Faculty of Medicine). The examination will be conducted in Swedish. Faculty examiner: Associate Professor Lars Ståhle (Department of Pharmacology, Karolinska Institutet (KI)).

Abstract
Aarnio, M. 2018. Visualization of Peripheral Pain Generating Processes and Inflammation in Musculoskeletal Tissue using [^{11}C]-D-deprenyl PET. *Digital Comprehensive Summaries of Uppsala Dissertations from the Faculty of Medicine* 1456. 72 pp. Uppsala: Acta Universitatis Upsaliensis. ISBN 978-91-513-0313-0.

An objective visualization and quantification of pain-generating processes in the periphery would alter pain diagnosis and represent an important paradigm shift in pain research. Positron emission tomography (PET) radioligand [11C]-D-deprenyl has shown an elevated uptake in painful inflammatory arthritis and whiplash-associated disorder. However, D-Deprenyl's molecular binding target and uptake mechanism in inflammation and musculoskeletal injuries are still unknown. The present thesis aimed to gain insight into the mechanisms of D-deprenyl binding and uptake and to verify whether pain-associated sites and inflammation in acute musculoskeletal injury could be visualized, objectively quantified and followed over time with [11C]-D-deprenyl PET-computed tomography (PET/CT).

To identify the D-deprenyl binding target, a high-throughput analysis and competitive radioligand binding studies were performed. D-deprenyl inhibited monoamine oxidase A (MAO-A) activity by 55%, MAO-B activity by 99% and angiotensin-converting enzyme (ACE) by 70%, which identified these enzymes as higher-affinity targets. Furthermore, radioligand receptor binding assays pointed favorably towards the concept of MAO-B as the primary target. To investigate the biochemical characteristics of the binding site, we used radioligand binding assays to assess differences in the binding profile in inflamed human synovial membranes exhibiting varying levels of inflammation. D-deprenyl bound to a single, saturable population of membrane-bound protein in synovial membrane homogenates and the level of inflammation correlated with an increase in D-deprenyl binding affinity.

To verify whether D-deprenyl can visualize pain-generating processes, patients with musculoskeletal injuries were investigated and followed-up with [11C]-D-deprenyl PET/CT. In the study of eight patients with ankle sprain, the molecular aspects of inflammation and tissue injury could be visualized, objectively quantified and followed over time with [11C]-D-deprenyl PET/CT. The pain coexisted with increased [11C]-D-deprenyl uptake. In the study of 16 whiplash patients, an altered [11C]-D-deprenyl uptake in the cervical bone structures and facet joints was associated with subjective pain levels and self-rated disability.

To further evaluate D-Deprenyl's usefulness as a marker of inflammation, three PET tracers were compared in an animal PET/CT study. Preliminary findings showed that [11C]-D-deprenyl had an almost identical uptake pattern when compared with [11C]-L-deprenyl. The two deprenyl enantiomers showed no signs of specific binding or trapping and therefore may not be useful to study further in models of inflammatory pain, surgical pain, or both.

This thesis demonstrates that D-deprenyl visualizes painful inflammation in musculoskeletal injuries and that the probable underlying mechanism of [11C]-D-deprenyl uptake is binding to MAO.

Keywords: ankle injuries, arthritis, binding site, binding target, carbon-11, deprenyl, high-throughput screening, inflammation, monoamine oxi-dase, pain, PET, whiplash

Mikko Aarnio, Department of Surgical Sciences, Anaesthesiology and Intensive Care, Akademiska sjukhuset, Uppsala University, SE-75185 Uppsala, Sweden.

ISSN 1651-6206
ISBN 978-91-513-0313-0
urn:nbn:se:uu:diva-347685 (http://urn.kb.se/resolve?urn=urn:nbn:se:uu:diva-347685)

Bene diagnoscitur, bene curatur

To Riina, Lukas, Ines and Ellen

List of Papers

This thesis is based on the following papers, which are referred to in the text by their Roman numerals.

I Lesniak, A., Aarnio, M., Jonsson A., Norberg, T., Nyberg, F., Gordh, T. (2016) High-throughput screening and radioligand binding studies reveal monoamine oxidase-B as the primary binding target for D-deprenyl. *Life Sciences*, 152:231–237

II Lesniak, A., Aarnio, M., Diwakarla, S., Norberg, T., Nyberg, F., Gordh, T. (2018) Characterization of the binding site for D-deprenyl in human inflamed synovial membrane. *Life Sciences*, 194:26–33

III Aarnio, M., Appel, L., Fredrikson, M., Gordh, T., Wolf, O., Sörensen, J., Thulin, M., Peterson, M., Linnman, C. (2017) Visualization of inflammation in acute and healing phases of traumatic ankle sprain using [^{11}C]-D-deprenyl PET/CT. *Scandinavian Journal of Pain*, 17:418–424

IV Aarnio, M., Linnman, C., Fredrikson, M., Lampa, E., Sörensen, J., Gordh, T. Whiplash injuries associated with experienced pain and disability can be visualized with [^{11}C]-D-deprenyl PET/CT. *Submitted for publication*

V Aarnio, M., Antoni, G., Hall, H., Ängeby Möller, K., Gordh, T., Sörensen, J. Evaluation of PET tracers [^{11}C]D-deprenyl, [^{11}C]L-dideuteriumdeprenyl and [^{18}F]FDG for Visualization of Acute i Inflammation in a Rat Model of Pain - Preliminary Findings. *Manuscript*

Reprints were made with permission from the respective publishers.

Contents

Abbreviations

[^{11}C]DDE	[^{11}C]-D-deprenyl
[^{11}C]DED	[^{11}C]-L-deprenyl
[^{18}F]FDG	[^{18}F]fluorodeoxyglucose
ACE	Angiotensin converting enzyme
ASIC	Acid-sensing ion channel
ATP	Adenosine triphosphate
BAT	Brown adipose tissue
B_{max}	Binding site density
CNS	Central nervous system
CROM	Cervical range of motion
CT	Computed tomography
DAMP	Damage associated molecular pattern
EFC	Enzyme fragment complementation
fMRI	Functional magnetic resonance imaging
FTA	Anterior fibulotalar ligament
GPCR	G-protein coupled receptor
GRPC	Calcitonin gene-related peptide
HRH1	Histamine receptor H1
HRH3	Histamine receptor H3
ID%	Percent injected dose
Kd	Dissociation constant
Ki	Inhibitory constant
MAO	Monoamine oxidase
MAO-A	Monoamine oxidase A
MAO-B	Monoamine oxidase B
MMP	Matrix metalloproteinase
MRI	Magnetic resonance imaging
NDI	Neck disability index
NGF	Nerve growth factor
PET	Positron emission tomography
PET/CT	Combined positron emission tomography/computed tomography
PPR	Pattern recognition receptor
ROI	Region of interest
ROS	Reactive oxygen species
SSAO	Semicarbazide-sensitive amine oxidase

SUV	Standardized uptake value
TACT	Time activity
TRP	Transient receptor potential
TRPA1	Transient receptor potential ankyrin 1
TRPV1	Transient receptor potential vanilloid 1
TSPO	Mitochondrial membrane translocator protein
UCP-1	Uncoupling protein 1
WAD	Whiplash associated disorder
VAP-1	Vascular adhesion protein 1
VAS	Visual analogue scale
VCAM-1	Vascular cell adhesion molecule
VOI	Volume of interest

Introduction

The International Association for the Study of Pain (IASP) first defined pain some 39 years ago in an editorial of PAIN® by Bonica1: "Pain is unpleasant sensory and emotional experience associated with actual or potential tissue damage, or described in terms of such damage"

According to this definition, pain is always a subjective psychological state that does not consider linking pain to the stimulus or to a clear pathophysiological cause. While common sense suggests that pain mostly has a physical peripheral or proximate physical cause, it is, per definition, only a sensation and is always an unpleasant emotional experience that our body has learned through evolution and through individual experiences to associate this sensation with actual or potential tissue damage. Again, in accordance with the definition, pain is a uniquely personal experience and, not surprisingly, subjective self-reports remain the gold standard of assessment. Unfortunately, these self-reports are influenced by many factors [2]. To only rely on self-reports is also partly against the principal of scientific objectivity in which the goal is to minimize personal and emotional biases. Without objective findings the patient may have to carry the burden: Pain can be neglected, misunderstood and under/misdiagnosed if the patient cannot communicate or give self-reports. There is also a risk that patients with chronic pain syndromes, where the exact pathophysiology is not fully understood, and no actual tissue damage is detectable with current methods, may be met with disbelief by health care professionals and insurance providers.

There is no direct causality between actual tissue injury and pain intensity and pain research has in the past years and decades concentrated on the central processing of the pain signal. The reasonfor this focus is that the advent of modern technologies (e.g., positron emission tomography, PET and functional magnetic resonance imaging, fMRI), has allowed functional imaging of the brain easy and accessible. At present, we do not know the precise role nociceptive signaling from the peripheral tissue plays and how much it contributes to the complex processes leading to a response in the cerebral "pain matrix". Therefore, an objective visualization, detection and quantification of pain-generating processes in the periphery would alter pain diagnosis and represent a paradigm shift in pain research. For one, the doctor would gain a better understanding of the pain pathophysiology and an objective diagnostic finding would bring us a step closer to ‘precision medicine’. Patients would receive support for their subjective self-report, and the scientist obtain help to re-focus

on the peripheral signaling as a 'driver' of peripheral and central sensitization. This, in turn, would facilitate diagnosis, clinical assessment and decisions as well as treatment monitoring.

We make no attempt to challenge the idea that the nociceptive signal from tissue injury must be connected or projected up centrally to be called pain. No do we claim that pain is the product of a linear sensory system without any modulations or interactions. In this summary, we try to focus on nociception, which can be defined as the detection of certain harmful or tissue-damaging stimuli and the subsequent transmission of encoded information to the brain. It is a physiological sensory process contrary to pain that is a subjective experience. In most cases it is the nociception that activates a perceptual process that is we call pain. Nociception is activated by a tissue injury (through trauma, surgery or inflammation), which generates the nociceptive impulses that propagate from the nociceptors and after a good deal of modulation in their path, reaches the brain and get notice.

Although tissue injury that induces inflammation plays a pivotal role in the generation of pain, few studies have localized and quantified the extent of peripheral injury and inflammation in pain patients with molecular imaging. In this thesis the potential of visualization and objective measurement of the pain-generating processes and inflammation in the periphery using PET/CT and a tracer [^{11}C]-D-deprenyl is investigated. The summary review of the literature helps the reader to understand certain aspects of the complex nature and close interactions between nociception and inflammation; however, te review is not meant to be exhaustive. We give particular emphasis to the mechanism of pain impulse generation in the periphery, processes underlying inflammation and inflammatory pain and the possible role of peripheral inflammation in chronic pain.

Pain

Anatomical overview of pain signaling pathways[3]

The transmission of nociceptive pain information starts with a stimulus that is an actually or a potentially tissue damaging event that is transduced and encoded by a receptor of the peripheral somatosensory nervous system called the nociceptor. The main cell body of this 'detector' is located in the dorsal root ganglia (or trigeminal ganglion) and it has a central axonal part (innervates spinal cord) and a peripheral part that innervates the target organ. The primary afferent fibers are pseudounipolar, i.e. the information is not carried uni-directionally but the axons are split into central and peripheral branches. This anatomical aberration makes it possible for proteins and other signal substances manufactured in the cell body to be distributed to both ends, along with messages that can be received and sent to both ends. However, both (peripheral and the central) terminals of the nociceptor can be activated and regulated by endogenous molecules (e.g., neurotransmitters), whereas only the peripheral terminal reacts to heat and mechanical stimulus. The nociceptors can be divided into two major classes[4]. The first class includes myelinated Aδ (conduction velocities of 5 to 30 m/s, 'first' or sharp pain) and Aβ fibers (33-75 m/s, light touch). Aδ nociceptors can be further divided into type I high threshold mechanical receptors (HTM) and type II nociceptors, which have a very high mechanical threshold but a considerably lower heat threshold. The second major class of nociceptors conveys poorly localized 'second' or slow pain and consists of unmyelinated C fibers (0.2-2 m/s). C nociceptors are polymodal, i.e. they perform more than a single function and are both heat and mechanically sensitive. From an inflammatory perspective, there are two populations of C fibers of particular interest. First, 'peptidergic' C fibers release substance P and calcitonin gene-related peptide (GCRP). Second, the silent C nociceptors come into action when the 'inflammatory soup' alters its function[5]. These Aδ and C neurons (primary afferents) convey and mediate the noxious information by activation of voltage-gated sodium channels and synapse with a second-order neuron in the dorsal horn of the spinal cord. Thereafter, the pain message is mainly carried through the spinothalamic and spinorethiculothalamic tract to the thalamus and brainstem, and after that to the final destination in the group of cortical structures of the brain where it is perceived (the somatosensory cortex for sensory discrimination and the anterior gingulate gyrus and insular cortex for emotional aspects) [6]. The pain signal can be modulated and regulated in several levels on its way from the dorsal horn to the pain perceiving centers in central nervous system (CNS), but this is out of the scope of this review.

The nociception and pain impulse generation

The nociceptor has specific transduction molecules to detect noxious stimuli and to relay that information by accomplishing an influx of calcium, potassium and sodium, which depolarizes the cell and generates an action potential that propagates to synapses in the dorsal horn. Each nociceptor subtype expresses its collection of these 'taste bud channels' and builds its ability to react to mechanical, thermal or chemical stimuli. The most important of these ion channels belong to the transient receptor potential (TRP) family. They can also detect chemical stimuli such as the capsaicin or vanilloid receptor (TRP vanilloid 1, TRPV1) [7] and the 'wasabi' receptor (TRP ankyrin 1, TRPA1)[8]. Aδ and C nociceptors are sensible to tissue-damaging temperatures through the TPRV-1 receptor[7] which clearly connects the receptor with pain. Particularly noteworthy is that the response of TRPV1 is enhanced, and it is activated by protons (low Ph), neurotrophins (nerve growth factor, NGF) and bradykinin[9] suggesting that this receptor can integrate the thermal and chemical proinflammatory stimuli. As the name implies, TRPV1 is activated by vanilloids, including capsaicin that is the component of chili pepper that makes it 'hot'. TRPV1 and TRPA1 are also located in peripheral non-neuronal tissue (e.g., blood, mononuclear cells, adipose tissue, fibroblasts and keratinocytes)[8], emphasizing their important function in infection and inflammation as a bridge between the inflammatory milieu in the extracellular matrix and the cell. TRPA1 is classically activated by mustard oil, other irritants and oxidative stress[10]. Endogenous TRPA1 agonists include hydrogen peroxide (H_2O_2) that is a byproduct of monoamine oxidases (MAOs) deamination of neurotransmitters. There are also other 'chemosensitive' ion channels and proteins that are activated and upregulated in inflammation, such as acid-sensing ion channel (ASIC) and Na_v 1.7. Voltage-gated sodium channel. Na_v 1.7 relay mostly thermal and mechanical signals[11] and ASICs are a voltage-independent proton-gated sodium-channel that is activated under acidic conditions or by a decrease in pH but also by mechanical stimulation[12].

Inflammatory pain

Inflammatory pain, a subtype of nociceptive pain, can be explained by increased sensitivity to pain that is associated with injury repair and healing[3]. Typical examples are pain from post-traumatic osteoarthritis, rheumatoid arthritis and gout. Tissue inflammation induces the release of inflammatory mediators by activated nociceptors and multiple non-neural cells that infiltrate into the injured area. Both immune cells and endothelial cells, keratinocytes and fibroblasts build the beforementioned inflammatory soup that leads to potentiating of peripheral nociceptor transduction molecules[13] and promotes increased expression of pronociceptive proteins (TNeFa, IL-1B, nerve growth

factor beta (NGF-β), extracellular proteases and protons)[14]. Everything becomes even more complicated with altered central pain processing. Moreover, there is no clear correlation between pain intensity and different measures of peripheral inflammation or even radiographic findings[15].

Musculoskeletal pain

Tissue acidosis is a common disturbance in inflammatory, non-inflammatory, and fatigue-induced musculoskeletal pain. Acids injected into muscle produce acute pain and primary and secondary hyperalgesia[16]. This acidic milieu is detected by ASICs that are localized not only in primary afferent fibers but also in muscle, synovium and immune cells. These ASICs play a significant role in postoperative pain[17]. As with other transduction molecules, ASICs are modified by various endogenous modulators[18]. The explanation for 'late onset' muscle soreness or secondary hyperalgesia after non-damaging exercise brings the nociception and immune cells together, where a depletion of macrophages prevents this fatigue-induced hyperalgesia, and probably resident macrophages play a crucial role by detecting acidosis and by releasing chemicals (e.g., proalgesic cytokines and ATP) to produce hyperalgesia[19].

Inflammation

Inflammatory soup and peripheral sensitization

'Chemo-nociception' is an important aspect of acute and persistent pain. Multiple different substances and chemicals (histamine, bradykinin, serotonin, prostaglandins, leukotrienes, potassium, glutamate, ATP and protons) are released into acutely injured tissue by cells of vascular origin, mast cells or from the injured cells. Soon afterward, other factors (both chemokines and cytokines, including interleukins-1(IL-1) and -6 (IL-6), interferon and tumor necrosis factor alfa TNFa), which have a vital role in the inflammatory processes, are released from cells of the immune system and by phagocyte cells. These pro-algesic substances build an extracellular milieu that is referred as inflammatory soup (or 'sensitizing soup')[20]. They have several and complex interactions that can activate the nociceptors directly or modify their responsiveness and activity by acting alone or in combination to modulate and lower the nociceptors threshold for mechanical, thermal or chemical stimuli. Modulation can act directly on the transduction molecules or by nociceptors downstream signaling pathways. This process is called peripheral sensitization, a phenomenon known since 1950[21,22]. Peripheral sensitization occurs most commonly from inflammation-derived changes in the chemical environment of the nociceptor; This process is different from the central sensitizing process [23,24], where central mechanisms lead to enhanced processing of pain messages. In any event, these two processes interact and are hard to separate, as enhanced nociceptive inputs from the injury site or the peripheral first order nerve injury alone contributes to the central sensitization[25].

Finally, the complexity of the peripheral pain generation with its multiple mediators, receptors and interactions is a logical reason why there is no 'magic bullet' or one substance that is sufficient to dramatically alter the level of pain in the periphery.

Sterile inflammation

Inflammation has five major clinical manifestations: rubor (redness), calor (heat), tumor (swelling), dolor (pain) and functio laesa (disturbed function). On the cellular or tissue level inflammation is characterized by an increase in vascular permeability and blood flow, activation of immune competent cells and infiltration of mobile cells of the immune system and cytokine production. The goal and evolutionary function of inflammation is to eliminate the cause of cell damage by taking the 'debris' and possible pathogens and promoting tissue repair and healing. The majority of inflammatory mediators act as a pro-

algesic substance and can bind to respective receptors or nociceptors. As we learned previously, the nociceptors can modulate inflammation by producing some of these inflammatory mediators themselves.

The sterile inflammatory reaction takes place in response to cell death or damage that is activated by non-microbial signals [26,27]. The pro-inflammatory responses are initiated by pattern recognition receptors (PRRs) on the cell surfaces of resident cells (tissue macrophages, endothelial cells, fibroblast and mast cells). PRRs sense damage-associated molecular patterns (DAMPs), which are endogenous factors usually hidden intracellularly (e.g., purines, ATP, uric acid and heat shock proteins). When cell membrane integrity is lost, these endogenous factors come into reach of resident cells, becoming indicators of tissue injury. The resident cells subsequently produce and release soluble mediators (complement, chemokines, cytokines, free radicals, vasoactive amines and prostaglandins) to guide activation and migration of leukocytes from the blood to the injured tissue. One of the mediators is bradykinin (angiotensin-converting enzymes (ACEs) break it down), which has direct algesic action but can also induce hyperalgesia after it is injected intramuscularly. When the initiating process has been cleared and is under control, resolution of the inflammation process starts. Nowadays, the resolution is known to be almost as complex and active as the onset of inflammation and where pro-resolution mediators regulate the process but also inhibit inflammatory pain[28]. Monocytes and macrophages that are not cleared or are still active release proinflammatory mediators (e.g., TNFa and IL-1β) that have been shown to induce enhanced pain conduction via modulation of transduction molecules (TRPV1, TRPA1, NAV 1.7-1.9)[29]. IL-1α and IL-1β are especially important in acute and chronic inflammation by facilitating nociceptors synaptic activity and signal transmission (as many other cytokines), and their receptors' overproduction is seen in osteoarthritis and neuropathic pain[30]. Incomplete resolution may be the reason to persistent inflammation ('the inflammation gone wrong'). However, it has not been adequately studied as to whether chronic inflammation is also as critical for persistent pain as acute inflammation is for driving acute pain. The prevailing belief is that chronic pain cannot be explained by peripheral inflammation.

Inflammation in osteoarthritis

As already noted, there is an overabundance of different inflammatory mediators that are released after tissue injury. In osteoarthritis, a low-grade inflammation is sustained and ongoing production of these inflammatory mediators can persist with leukocyte infiltration[31]. The leading group of leukocytes in osteoarthritis has been shown to be macrophages and T-lymphocytes[32]. Activation of synovial cells and chondrocytes is an important part of the sustained inflammation and osteoarthritis pathogenesis. These cells produce multiple

chemokines, which after binding to cell surface chemokine receptors promote cellular motility by helping leukocytes to migrate to sites of tissue damage. They also recruit other cells to sites of tissue repair. Studies suggests that molecules released during tissue damage can activate nociceptive pathways through PRR dependent chemokine production[33]. Not surprisingly, the chemokine receptors are involved in neuropathic pain and neuroinflammation[34].

Tissue injury

Tissue injury and healing

After an injury, the tissue goes through a predictable sequence of events. The intensity and extent of these complex events depend on the injury mechanism and the amount and type of cells that are damaged. As was mentioned earlier, necrotic and damaged cells in tissue injury leak DAMPs to extracellular space, which triggers an inflammation and healing process with the goal to replace the damaged cells by living cells through granulation and regeneration. A minimal injury can be contained locally but when this is exceeded, a larger recruitment and activation of multiple inflammatory and repair cells occur. This recruitment is a chemically mediated amplification cascade with the complex molecular interaction between different cells and substances. Such recruitment range from small undetectable injuries to the life-threatening systemic inflammatory response after a major trauma[35]. Dysregulation or interference of the normal healing process results in chronic inflammation, pain, excessive fibrosis and pathological scar formation.

Tissue injury and the healing process can be divided into several stages or 'phases'[36-39]. These phases are interlinked considerably and act as an initiator to the next phase:

I Degeneration/hemorrhagic stage/hemostasis (4-6 hours): Platelets are not only important in hemostasis but also once they become activated, they degranulate and release cytokines and growth factors. The clot also provides a 'matrix scaffold' for the recruitment of inflammatory cells.

II Inflammatory stage (24 hours-2 weeks): Macrophages and neutrophils invade the area of tissue injury and begin the phagocytosis of 'debris'. High concentrations of proinflammatory cytokines and substances increase the activity of these cells. This phase has a rapid onset (hours), reaching its peak activity after 1-3 days until gradually diminishing during the next few weeks. This phase is an essential component of healing and not a pathological response to trauma.

III Proliferative stage (24 hours-4 weeks): Extrinsic cells migrate and increase in numbers in the area of tissue injury and start to form an immature granulation tissue. This phase also has a rapid onset, but it takes a few weeks to reach its peak activity when the bulk of granulation tissue is formed. The phase decreases slowly (from 1 week to several months). The injured tissue is continuously hypercellular.

IV Remodeling phase (1-2 weeks-2 years): The maximal physiologic strength of the tissue is brought back. For example, in this 'maturation phase', collagen III is replaced by more resistant collagen I. However, complete regeneration hardly ever takes place and injured tissue never gains its pre-injury strength.

Inflammatory response to tissue injury

The inflammatory events are primarily the same whichever 'insult' initiates it (see page 19, phase II). Tissue damage results in two simultaneous responses. First, in a vascular response endothelial cells produce chemical mediators responsible for the permeability changes (histamine, bradykinin and serotonin). Second, in a cellular response, there is an early migration of phagocytes (neutrophils and macrophages) followed later by other immune cells. These cells, which act as 'debriders' work in a complex inflammatory environment with several substances and chemical mediators. Neutrophils are the most abundant cell type within 24 hours, but after that, their number is decreased and macrophages start to increase[40]. The magnitude of inflammation has a direct impact on scar formation by inducing excessive fibrosis and even slowing the repair process[41].

Whiplash injury

Neck injury (also referred to as whiplash injury) is classically a result from a rear-end motor vehicle collision where the individual is exposed to an acceleration-deceleration mechanism and to energy transfer that affect the neck and head[42]. Even though the injury may be relatively mild, these persons can develop chronic and persistent pain in which the injury consequences and symptoms do not only consist of neck pain, stiffness and headache but also of multiple different symptoms (e.g., dizziness, visual and auditory disturbances, shoulder and back pain, sleeping problems, motor dysfunction, central pain sensitization and cognitive impairment)[43,44]. This variety of symptoms and clinical manifestations is called whiplash associated disorder (WAD).

WAD is a globally important clinical, social and financial pain problem[45]. In Western countries, the prevalence of chronic WAD (persisting symptoms after 6 months) has been estimated to be as high as 1%. It has also been estimated that about 20% (14-40%) of patients after whiplash injury develop chronic pain and that 5-10% of them have severe constant pain[46]. The annual incidence of acute WAD has ranged from 0.8–4.2 per 1000 inhabitants[44]. In Sweden the overall incidence of WAD has been calculated to 2.3 per 1000 inhabitants[47] and the cost to society of whiplash injuries sustained in the

course of only 1 year has been estimated to 5.4 billion SEK or 640 million USD (calculated to equivalent worth year 2015)[48].

The symptoms of WAD are well known but the pathogenetic mechanisms and etiology of this disorder is still unclear and no certain peripheral pathology can unequivocally be detected with x-ray or MRI[49,50]. The development of chronic symptoms after whiplash injuries may also be influenced by psychological and social factors[51,52]. Moreover, central pain sensitization and hypersensitivity play an important role in the symptomatology. All this has led to a discussion of whether tissue damage is even needed to initiate or maintain WAD or that the syndrome itself is induced by society and by physicians[53,54].

Monoamine oxidase

MAO is a flavin-containing mitochondrial enzyme, which oxidizes (deaminates) monoaminergic neurotransmitters, other biogenic amines and for the body foreign chemical substances. It is located in the outer mitochondrial membrane but is also found in the cytosol. By deaminating biogenic amines (epinephrine, norepinephrine, serotonin, dopamine, benzylamine, tyramine and phenylethylamine), it is preventing those amines from entering the extracellular matrix and circulation. Thus, the MAO enzyme regulates biogenic amine tone in tissues.

In a MAO driven reaction the substrate is oxidated, where a corresponding aldehyde, H_2O_2 (hydrogen peroxide) and ammonia is produced:

$$RCH_2NH_2 + O_2 = RCHO + H_2O_2 + NH_3$$

MAO occurs in two isoforms, MAO-A and MAO-B, which are present in almost all brain regions and peripheral organs. Actually MAO is found in every cell type that contains mitochondria. MAO-A shows greater activity towards metabolism of serotonin and norepinephrine, whereas MAO-B breaks down benzylamine and phenylethylamine. Both isoforms metabolize dopamine. For a still unknown reason often only one subtype of the enzyme is predominated in a specific organ and within a specific cell, and there are differences between species[55,56]. For example, human platelets, granulocytes, lymphocytes and microglia (resident macrophages in the CNS) contain almost only MAO-B[57,58].

These biogenic amines have an important role in the control of analgesia. For example repeated reserpine injections (this depletes amines) in rats cause dysfunction of pain control in the CNS and hypesensitivity[59]. The byproduct of amines metabolism H_2O_2 is a highly active reactive oxygen species (ROS) and has been related to age-induced mitochondrial and cellular damage, parkinsonism and aging[60]. Many studies done on L-deprenyl suggest an antioxidative and anti-apoptotic activity, which is neuroprotective and not related to MAO-B inhibition.

Although MAO is expressed in the immune cells, its exact role in inflammation is not entirely clear. We do know that its metabolite H_2O_2 is an important signaling molecule that promotes inflammation[61]. In inflammation MAO-A is one of the signature genes that is modified by interleukins and the expression of the enzyme is strongly upregulated in activated monocytes and macrophages[62-64]. Furthermore, glucocorticoids and intermittent hypoxia induce MAO-A expression but have minimal effects on MAO-B[65,66]. Another example of MAOs importance in inflammation is semicarbazide-sensitive amine oxidase (SSAO) that has an enzymatic function but is also an inflammation-inducible adhesion protein that is better known as Vascular adhesion protein 1 (VAP-1)[67]. According to the literature, it can be assumed that a more MAO-A selective ligand would be a more useful marker of peripheral inflammation.

Deprenyl

Deprenyl is a pharmacological substance that was first synthesized in 1964 by Dr. Joseph Knoll et al.[68,69] The molecule was designed to be a psycho energizer (thought to lift state of mind) by combining amphetamine (psychostimulant) and pargyline (MAO inhibitor with antidepressant effects) in the same molecule. From 30 different molecules was the (-) enantiomer of E-250 (L-Deprenyl) was chosen. It was shown that this molecule (now better known as Selegiline) was the first selective MAO-B inhibitor free of the 'cheese effect'[70]. L-Deprenyl is nowadays included in treatment protocols for Parkinson´s disease (PD) and has also shown promise of neuroprotection and slowing the progression of PD. (-)-L-deprenyl is a 'suicide inhibitor' of MAO with a selectivity for MAO-B vs. MAO-A (234:1)[71]. Its binding leads to the diminished metabolism of monoamines. It is a lipophilic weak base that quickly penetrates tissues easily and possesses complex pharmacological activities and several possible bindings sites. Totally there are hundreds of different manuscripts published about (-)-L-deprenyl but only a few about (+)-enantiomer D-deprenyl. D-deprenyl is 25-500 times less potent MAO-B-inhibitor than its mirror isomer L-deprenyl[68,71]. Very little is known about its binding sites in the inflamed peripheral tissue. [^{11}C]-D-deprenyl uptake is hypothesized to be trapping in low pH regions, as demonstrated by lysosomotropic agents or binding to specific, still unknown, molecular structures[72]. D-deprenyl also suppresses electron flow in the respiratory chain in mitochondria, can initiate anti-apoptotic processes and has free radical scavenging action[73-75]. D-deprenyl is a potent dopamine uptake inhibitor and binds to the active dopamine transporter *in vitro*[76]. Both deprenyl isomers are metabolized stereoselectively, meaning that D-deprenyl is metabolized to D-amphetamine (four times more potent than L-amphetamine!), D-methamphetamine and D-desmethylselegiline[77]

The biological and medical importance of MAOs has created a surge to develop PET radiotracers to investigate their activity. Among the first to be labeled was L-Deprenyl. At Uppsala University, PET studies with deprenyl started already in the mid-1980s. In the beginning, the interest centered on dopamine receptors, especially concerning the uptake and metabolism of dopamine, which brought attention to MAO-B in the human brain. In these studies [^{11}C]-D-deprenyl was used as an MAO-B 'inactive' control for [^{11}C]-L-deprenyl[78,79]. In these brain studies [^{11}C]-D-deprenyl was found to incidentally elevate elevate uptake in painful shoulder joints and in certain pituitary tumors, which led to the hypothesis of D-deprenyl trapping in inflammation. These studies were later followed by a study on knee joint inflammation[72] and some unpublished pilot studies in the late 1980s. However, because of personnel and organizational changes, the intriguing properties of D-deprenyl were forgotten for more than decade.

Mitochondrion

The mitochondrion is a 0.5-1 μm long cell organelle that has three essential functions: bioenergetic, biosynthetic and signaling. Mitochondria act as 'powerhouses' of the cell by producing the energy carrier molecule adenosine triphosphate (ATP). They further generate the intermediary metabolites for synthesis and regulation of many macromolecules and communicate their 'biofitness' to the rest of cell[80,81].

Mitochondria are surrounded by two major membranes (the inner forming the characteristic folds) with a small intermembrane space between. Mitochondria have their own small maternally inherited genome[82], but as approximately 1500 mitochondrial proteins are involved in the complex function of this organelle, these protein are mostly encoded by the nuclear genome[83]. All the outer membrane proteins are synthesized in the cell cytoplasm and transported to the mitochondria (e.g., MAO-A and MAO-B). The present theory behind the origin of mitochondria is that an ancient nucleated cell ingested a prokaryotic cell (bacteria that later developed into mitochondria) and established a symbiotic relationship where the host cell guaranteed a protective environment for the engulfed mitochondria, which in turn, fulfilled the energy needs of the cell[84,85].

A result of this relative independency is that mitochondria, which can vary in shape and size, can divide and replicate independently from the cell. This division of mitochondria is stimulated by increasing energy-demand and therefore cells that have high energy need to contain more mitochondria[86]. Examples of these power-hungry cells with high amount of mitochondria are liver cells, muscle cells and brown adipose cells (compared with white adipose cells). An important aspect of this thesis is that a molecule that binds to MAO is not only a marker of the outer mitochondria membrane (amount and size of mitochondria) but also a marker of mitochondrial activity[63]. Mitochondria are also the major site for generation of ROS and free radicals[87], where MAO plays a key role.

Brown adipose tissue

White adipose tissue´s is specialized to energy storage but also has metabolic, neuroendocrine and immune functions[88]. In contrast, the main function of brown adipose tissue (BAT) is basal and inducible non-shivering thermogenesis. It simply increases energy expenditure and heat by burning fatty acids[89]. The heat is generated by uncoupling the oxidative phosphorylation in the mitochondrial inner membrane by the protein UCP1 (uncoupling protein 1) which is stimulated by the sympathetic nervous system[90]. BAT´s brownish color comes from the many mitochondria (which contain ferritin and heme

cofactors that gives the color to mitochondria). When compared with white adipose tissue, BAT is well vascularized and have less volume of cytoplasmic lipid droplets. In rodents, BAT is present throughout their lifespan but in human it was believed before 2007 that active BAT is basically nonexistent in adults and only found in children (especially newborns)[91] . Recent papers, however, have reported BAT in up to 80% of patients with locations mainly limited to lower neck and shoulder regions[92,93]. Interestingly, the mass and activity of BAT is greater in females and outdoor workers and the amount of BAT reduces with age. Furthermore, it varies with seasonal outdoor temperatures[94]. It has been shown in humans that an increased [^{18}F]FDG uptake in cervical regions by BAT can be a potential source of false positive PET scans[95,96]. It has also been speculated that [^{11}C]D-deprenyl retention resides in adipose tissue near deep cervical muscles[97].

Positron emission tomography (PET)

PET is a non-invasive diagnostic imaging technique with clinical applications that provides information about the function of the body and specific organs on a molecular and biochemistry level *in vivo*. This method takes advantage of biologically important compounds that are labeled with short-lived radionuclides without altering or interfering with biological activity. The specific radioactivity of these tracers is so high that the amount of ligand is minimal such that only an insignificant fraction of the target enzyme or receptor is occupied[78]. In practice, this means that PET offers functional and molecular information with high sensitivity in the nano-, pico- and micromolar range. In this project, the molecules were labeled with ^{11}C ($t_{1/2}$=20.4 min) or ^{18}F ($t_{1/2}$=109.8 min). PET radionuclides decay by the emission of a positron (β^+, which is a positive charged electron and antimatter to electrons) which travel until it combines with a free electron. The rest masses of the positron and electron are then converted to electromagnetic radiation in a coincident annihilation and two 511 keV gamma ray photons travel 180 degrees in opposite directions. These are recognized by the PET scanner which has a cylindrical assembly of radiation detectors in a ring-like structure. After signal processing, by reconstruction and acquiring serial PET images, it is possible to obtain quantitative information by determining the radioactivity concentration in the tissue of interest, as well as radiotracer kinetic behavior.

PET in inflammation

PET is increasingly used to diagnose, characterize and monitor disease activity in peripheral inflammatory disorders of both known and unknown origin [98-100]. In the future, PET will play an increasing role in identification and assessment of both infectious and inflammatory diseases (e.g., musculoskeletal infections, infected vascular grafts, rheumatoid arthritis, vasculitis and fever of unknown origin (FUO). The accumulation of PET radiotracers in inflamed tissue is based on four different mechanisms[101]:

I Metabolic activity of inflammatory cells: Glucose metabolism (fludeoxyglucose (FDG)) and choline metabolism (choline).

II Membrane markers of inflammatory cells: Translocator protein (TSPO), which has a high expression in leukocytes, activated microglia and astrocytes; somatostatin receptor in lymphocytes and macrophages and cannabinoid type 2 receptor in microglia.

III Inflammatory cytokines: Cyclooxygenases, MMP (matrix metalloproteinases), IL-2 and TNF-α.

IV Targets on inflammation-related vessels: Integrilin receptor, VAP-1, VCAM-1 (vascular cell adhesion molecule 1) and vessel permeability (albumin).

V In most cases, the mechanism would be a combination of unspecific accumulation at the sites of the inflammation as a result of both increased blood flow and vascular permeability and where local trapping and binding play a variable role[99].

Technical limitations of PET

In practice, the human PET scanner cannot resolve point sources smaller than 4-5 mm (X-ray computed tomography (CT) scanners < 1 mm and animal or pre-clinical PET scanner ~1mm). PET has some fundamental effects (positron range, detector width and acollinearity) that limit theoretical spatial resolution to a maximum of > 1.83-2.36 mm in clinical, and > 0,67-0,83 mm in pre-clinical PET cameras[102]. Therefore, as in this thesis, a combined system with x-ray CT (PET/CT) is normally used in which superimposed and co-registered CT images with their higher resolution add precision to the anatomical localization of regions identified on PET tracer uptake images[103]. The latest development is PET/MRI, which has much lesser ionizing radiation and a much better soft-tissue contrast as compared with CT.

Aims and questions

The overall purpose of my thesis was to investigate whether pain-generating processes in the periphery are possible to visualize and follow up objectively by using PET and D-deprenyl. We also explored the possible binding mechanism of D-deprenyl in peripheral tissue.

The specific aims according to each paper were as follows:

Paper I: To investigate and search for possible D-deprenyl binding sites.

Paper II: To characterize the binding properties of D-deprenyl in synovial membrane samples extracted from patients with knee joint arthritis. Can the radioligand differentiate the severity of inflammation between patients and is this effect related to MAO activity?

Paper III: To verify in patients whether pain associated sites and damage or inflammation extent in acute musculoskeletal injury (ankle sprain) could be visualized, quantified and followed over time with [^{11}C]-D-deprenyl as a PET radioligand. Is [^{11}C]-D-deprenyl uptake acutely elevated and localized to injured structures, reduced as a function of healing and correlated with subjective pain experience?

Paper IV: To characterize acute alterations and the predictive ability of [^{11}C]-D-deprenyl uptake for whiplash signs and symptoms at a 6-month follow-up. Is [^{11}C]-D-deprenyl uptake acutely elevated in a whiplash injury, localized to anatomically relevant injured tissues, colocalized to tender points and correlated with subjective pain experience? Would patients with persistent pain have prolonged elevated [^{11}C]-D-deprenyl uptake at the injury sites at follow-up?

Paper V: To further investigate the usefulness of [^{11}C]-D-deprenyl as a marker of inflammation and compare the uptake of [^{11}C]-D-deprenyl with its stereoisomer [^{11}C]-L-deprenyl (selegiline) and [^{18}F]FDG (the most widely used PET tracer for imaging inflammation) in a rat model of monoarthritis in ankle joint and in a rat model of surgical pain with lesions in skin, muscle and bone. Is it possible to study radioligands for inflammation in these two animal models?

Materials and methods

Patients

In Paper II, 30 elective knee replacement surgery patients diagnosed with either rheumatoid arthritis (n=19) or osteoarthritis (n=11) were included in the study.

In Paper III, eight otherwise healthy patients with an acute unilateral traumatic ankle sprain, were studied. Traumatic ankle sprain was chosen as a musculoskeletal trauma model because of its simplicity in diagnosis, examination, the healing process and most importantly because the intact ankle could be used as a control. The patients were recruited from the emergency department at Uppsala University Hospital, Uppsala, Sweden and diagnosed by an orthopedic surgeon.

In Paper IV, 16 patients with a whiplash injury grade II after a car accident were recruited from the same emergency department as in Paper III. Eight healthy pain-free subjects from a previous study were included as controls[97].

All three studies were approved by the Ethics Committee of the Faculty of Medicine at Uppsala University, Sweden (Papers III and IV were also approved by the Radiation Ethics and Safety Committee of Uppsala University Hospital, Uppsala, Sweden). Informed consent was obtained from all study participants.

Animals

In paper I, 10 adult male Sprague-Dawley rats, weighing approximately 250 g, were used for the *in vitro* binding studies. Rats were sacrificed by decapitation and the brain without cerebellum was used.

In paper V, 14 Adult male Sprague-Dawley rats, weighing approximately 300 g, were used for the tracer evaluation study. The reason for using rats was twofold. First, an important goal of the study was to develop an experimental animal model in which comparison of PET tracers for pain and inflammation could be used and the research group had already knowledge and methodology of the two experimental rat models that were used. Second, we had the possibility to use animal PET/CT scanner (most suitable for rodents such as rat and mouse) for the studies.

In both studies the treatment of the animals and the PET investigations were approved by the Uppsala Ethical Committee on Animal Experiments. All rats were handled in accordance with the guidelines of the Swedish National Board for Laboratory Animals and the European Convention on Animal Care.

High throughput screening (Paper I)

High Throughput Screening (HTS) is an automated process that can be used to quickly assay the ligand against hundreds of receptors, enzymes, ion-channels or other pharmacological targets for binding and functional activity. We used a commercial *gpcr*MAX™ GPCR Assay Panel developed by DiscoverX™ (Fremont, CA, USA) that used the PathHunter™ β-arrestin recruitment enzyme fragment complementation (EFC) technique to assess functional interactions of D-deprenyl with 168 G-protein-coupled receptors (GPCR) covering over 60 receptor families. Potential 'hits' were identified based on the agonist or antagonist activity of a single dose of D-deprenyl (10μM) towards each GPCR. D-deprenyl was also screened against its inhibitory activity towards 84 enzymes with the use of a commercial EnzymeprofilingScreen™ package provided by Eurofins Cerep Panlabs, INC(Redmond, WA, USA). This screen employs an array of methods that have been adapted from the scientific literature (www.eurofinspanlabs.com).

Radioligand binding studies (Papers I and II)

Testing how two molecules interact with each other is a common procedure in cellular and molecular biology. In radioligand binding studies (reviewed by Pollard 2010 and Hulme and Trevethick 2010)[104,105] the objective is not solely to investigate the mechanism of interaction between different molecules and the potential binding sites, but also to quantify the interaction by giving a measure of affinity (how strong the binding is). The objective of the study was to find the yet unknown target for deprenyl in rat brain mitochondrial or whole cell fractions and in inflamed human synovium.

The key molecular principle and the simplest model for understanding binding studies is when a ligand (radioligand) binds to a binding site (a receptor or protein) and forms a complex. This is a reversible process that occurs until equilibrium is reached:

[*radioligand*] + [*binding site*]↔ [*radioligand·binding site*]

At equilibrium are the forward and reverse reactions equal:

[*radioligand*] x [*binding site*] x K_{on} = [*radioligand·binding site*] x k_{off}

where the rate of the association is k_{on} and the rate for the dissociation is k_{off}. The formula can be rearranged to $k_{off} / k_{on} = [radioligand] \times [binding\ site] / [radioligand{\cdot}binding\ site] = K_d$

One of the main goals of binding studies is to measure the dissociation constant at equilibrium (K_d) or the inhibitory constant (K_i), which are the most commonly used measures to describe ligand affinity.

In classical competitive binding assay, a single concentration of a radioligand (in this case [H^3]-D-deprenyl) competes against multiple concentrations of another unlabeled (or 'cold') molecule. The objective is to determine IC_{50}, the concentration of cold ligand that inhibits 50% of the radioligand binding. From IC_{50} you can mathematically derive apparent affinity (K_i).

$K_i = IC_{50} / (1 + [ligand\ concentration] / K_d)$

The basic principle of competitive binding assays used is to let a fixed concentration of [H^3]-D-deprenyl (around its K_d) to compete with a wide concentration range of different well-characterized ligands specific for a putative target for D-deprenyl. The concentration of [H^3]-D-deprenyl was chosen so that less than 10% of added radioligand is bound to the target, thus preventing radioligand depletion. One can then assume that the [*testligand·binding site*] is smaller than [*testligand*] concentration and consequently [*testligand*]free = *[testligand*]total added. This means that the binding study can be reduced to measuring the fraction of bound [H^3]-D-deprenyl as a function of the free testligand concentration. The competing ligands are thought to bind to the same binding site, so the test ligand is considered here as a competitor for [H^3]-D-deprenyl, and IC_{50} gives a concentration at which [H^3]-D-deprenyl is inhibited by 50%. In Paper I, however, the K_d and binding site density (B_{max}) were computed from a homologous competitive binding assay instead of a saturation binding experiment. This was based on the assumption that [H^3]-D-deprenyl and unlabeled D-deprenyl have identical affinities for the unknown binding site and thus K_d and K_i values are identical.

$K_d = K_i = IC_{50} - [ligand\ concentration]$

$B_{max} = [curve\ top - curve\ bottom] \times [ligand\ concentration] / K_d + [ligand\ concentration]$

In Paper II, kinetic experiments were performed to estimate the Kd of D-deprenyl and determine the incubation time to reach equilibrium in inflamed human synovial homogenates. In these experiments the association (k_{on}) and

dissociation (k_{off}) rates of [H^3]-D-deprenyl were determined. As was mentioned earlier, the ratio of these constants provides an independent estimate of K_d.

$k_{on} = (k_{obs}\text{-}k_{off}) / [\textit{radioligand concentration}]$
$K_d = (k_{off} / k_{on})$

The value of k_{obs} is determined in an association experiment where a fixed radioligand concentration binds to the target site until equilibrium is reached. The value of k_{off} is determined in a dissociation experiment where excess of unlabeled ligand is added after reaching equilibrium and radioligand dissociation is measured over time. After plotting $\ln[B_{eq}/B_{eq} - B_t)]$ and $\ln[(B_t/ B_{eq})]$ against time where B_{eq} is the amount of radioligand bound at equilibrium and B_t is the amount of radioligand bound at respective time points, it is possible to calculate k_{obs} and k_{off}.

Subjective ratings and clinical assessment of pain and disability (Papers III and IV)

Immediately before each examination of the patients the locations of maximum tenderness were palpated and marked on an anatomical picture. The patients rated their current subjective pain levels on a visual analogue scale (VAS), ranging from 0 (no pain) to 10 (worst imaginable pain). In Paper IV, a cervical range of motion (CROM) goniometer (Performance Attainment Associates, Roseville, MN) was used to measure the six active movements of the neck[106]. Also in Paper IV, the patients rated how much the neck pain affects their ability to manage everyday activities by completing a short neck disability index (NDI) questionnaire[107], with scores ranging from 0 (no activity limitation) to 50 (complete activity limitation).

PET/CT scanning and data analysis in the patient studies (Papers III and IV)

All patients were investigated with a GE Discovery ST PET/CT scanner (General Electric Medical Systems, Milwaukee, WI, USA) with an axial field of 15.7 cm. Patients were in supine position in the scanner with the studied anatomical region gently fixed and positioned in the scanner field. For the PET data analysis and for identification of the lesions and to limit the effects of blood flow a summation image was created from the last two frames of the dynamic PET emission data (25-45 min post-tracer administration). In paper IV a static data, (45-60 min) were also used to analyze lower neck regions. A

volume of interest (VOI) was delineated manually so that it contained the visually evident tracer uptake. This procedure was repeated in every investigation and the CT was used to define and localize the anatomical regions. CT was also used to delineate the anatomical reference and control regions. From these VOIs, time activity (TACT) data were generated for all scans from each patient, which represented the dynamic sequence of radioactivity levels for the VOI in each PET/CT scan from 0-45 min. The TACT data were standardized on the administered dose of radioactivity and the patient's body weight, resulting in a standardized uptake value (SUV), with the equation [108].

SUV = [activity (Bq/ml) x body weight (g)] / total injected dose (Bq).

From the SUV calculations, the average SUV value (SUV_{MEAN}) was defined as the mean voxel value in a specific VOI and the maximum SUV value (SUV_{MAX}) was defined as the highest value observed in a specific VOI. Subsequently, the SUV_{RATIO} was defined for each region as the ratio of SUV_{MEAN} between the injured foot and the non-injured foot (Paper III) and as the ratio of SUV_{MAX} between the anatomical region or lesion and the cerebellar reference region (Paper IV).

Anesthesia and preparation (Paper V)

In the rat model of monoarthritis the animals (10 rats) were anesthetized with a volatile anesthetic (3% isoflurane) and injected with 50 µl Freund's complete adjuvant into the left ankle joint[109]. In the rat model of musculoskeletal injury, four rats were anesthetized with 3% enflurane and the surgical procedure started on the plantar aspect of the left hind paw. A 1.5-cm longitudinal incision was made through the skin and fascia and after that the elevated plantar muscle was cut longitudinally before the skin was sutured. The procedure was finished by drilling a perpendicular hole (1 mm diameter and 5mm deep) percutaneously through the calcaneus bone of the same hind paw[110]. The procedures took only a few minutes (injection 30 s) and rats recovered from the anesthesia within 3-5 min. The rats were investigated in the PET/CT scanner 3 days after the procedures when the inflammation should have been most prominent. The radioligand was administered as a bolus in the tail vein while the animal was in the PET camera. At the end of the experiment, the rat was sacrificed under sodium penthothal anesthesia.

PET scanning and data analysis in the animal study (Paper V)

The rats were anesthetized (3% isoflurane in 40% oxygen/60% breathing air) and immediately put on a warm camera bed and covered with cloth or plastic to reduce the loss of body temperature during the experiment. Imaging was performed on a GE Triumph animal PET/SPECT/CT scanner. The scan time was set to 40 min for the ^{11}C labeled tracers and 60 min for [^{18}F]FDG. For the PET data analysis regions of interest (ROIs) were drawn on the PET image covering the total of each ankle joint. Next, time activity curves were generated. In this study, data in percent of activity in the region of interest of a given dose (ID%) were used instead of SUV values. It was done because of differences in hind paw size.

Statistical methods

In Papers I and II radioligand binding data were fitted with nonlinear regression analysis. K_d and Ki constants were expressed as means ±95% confidence intervals (CIs) and receptor density (Bmax) was reported as mean ± SEM. Affinity comparisons were performed with the extra sum of squares F test. In Paper II, to determine the differences in binding density and affinity between samples one-way analysis of variance (ANOVA) was performed, followed by Dunnett's post-hoc test for multiple comparisons.

In the Papers III and IV, the differences in SUV-related measurements were evaluated with Wilcoxon's signed-rank test and correlations between SUV-related measures and subjective ratings were assessed with Spearman's rank order test. This test was done because of the small sample size that is typical of PET pilot studies and that we could not assume a normal distribution. Normally, sample size calculation is not needed (or possible) in pilot studies and it had been difficult to justify ethically or for patient safety concerns (radiation) a larger sample size when the patients were 'healthy' volunteers who did not have any individual medical or diagnostic benefit from these pilot studies.
In Paper III, subjective pain ratings and elevated uptakes were also dichotomized (presence vs. non-presence) for both feet. The dichotomized data were analyzed using a mixed logistic regression model[111]. To analyze the pairwise correlations between uptake and subjective ratings, a multivariate rank-based association test was performed in Paper IV to formally test for associations adjusting for multiple comparisons[112].

In Paper V, data were expressed as mean values of ID% ± SEM and Wilcoxon matched-pairs signed rank test was used to determine differences between binding.

Results from Paper I

High-throughput screening

HTS revealed no evident D-deprenyl targets among the 165 GPCRs analyzed. However, histamine 1 (HRH1) and histamine 3 (HRH3) surfaced as receptors to which D-deprenyl demonstrated the highest antagonistic activity (42% for HRH1 and 20% for HRH3).

Contrary to GPCRs, three putative binding sites for D-deprenyl were identified among 84 enzyme targets. D-deprenyl inhibited MAO-A activity by 55%, MAO-B by 99% and ACE by 70%.

Radioligand binding

[^{3}H]-D-deprenyl competitive binding experiments in rat brain mitochondria revealed that selegiline readily inhibited [^{3}H]-D-deprenyl binding with a Ki value of 6.2 ± 0.11 nM. Similarly, D-deprenyl also competed for the same site as selegiline, but with a 37-fold lower affinity (Ki=230 nM). A specific MAO-A inhibitor (pirlindole mesylate) showed considerable lower affinity (Ki=9.2 µM). Captopril (ACE inhibitor) did not displace [^{3}H]-D-deprenyl binding in rat brain whole cell preparations and showed a very low predicted affinity of 51.4 µM (Figure 1).

Neither of the HRH21and HRH3 agonists competed with [^{3}H]-D-deprenyl for binding in whole cell rat brain homogenates.

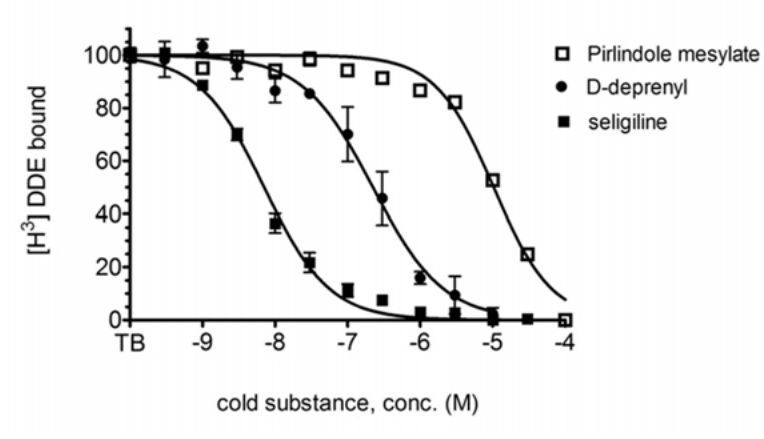

Figure 1. Competition curves showing [^{3}H]-D-deprenyl ([^{3}H]DDE) displacement by specific MAO inhibitors. Rat brain mitochondrial fraction was incubated with 10nM [3H]-D-deprenyl in the presence of (□) pirlindole mesylate (MAO-A inhibitor), (■) selegiline (MAO-B inhibitor) and (●) D-deprenyl.

Results from Paper II

[^{3}H]-D-deprenyl binding site density and affinity

There were no differences in [^{3}H]-D-deprenyl binding site density in inflamed synovial membrane between samples of varying degree of inflammation. K_d calculated from the homologous competition experiments was 61.4 nM (95% CI 41.9-90.1) and from the kinetic experiments 64 nM. However, significant differences in binding affinity of [^{3}H]-D-deprenyl (K_d) were detected between grade 0 synovial membrane preparations and grade 1, 2 and 3 synovia. Significant group differences were also found in the binding potential (BP) as grade 2 and 3 synovia showed an elevation in BP compared with grade 0 synovia (Figure 2). In competitive binding experiments L-deprenyl (selective MAO-B inhibitor, selegiline) dose-dependently inhibited [^{3}H]-D-deprenyl binding with a nanomolar affinity whereas pirlindole mesylate (selective MAO-A inhibitor) did it with a macromolar affinity. Contrary to D-deprenyl, the binding affinity of these two inhibitors did not differ between samples of different inflammation grades (Figure 3).

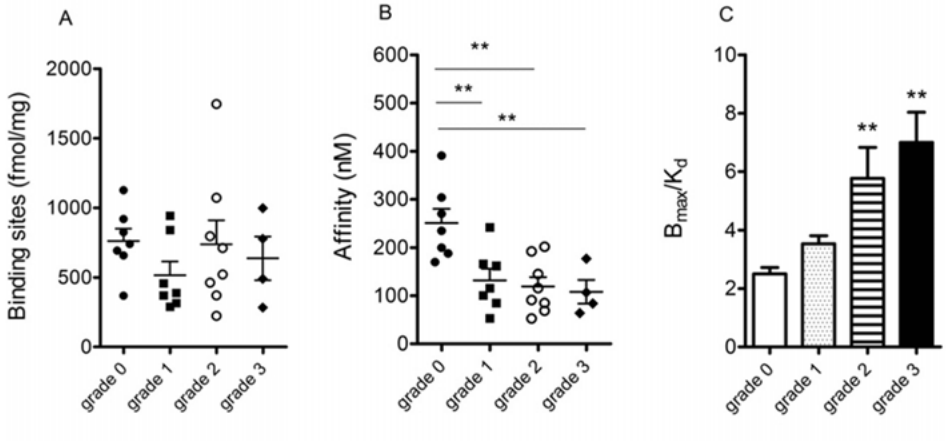

Figure 2. Binding site density (A) affinity (B) and binding potential (C) of [^{3}H]-D-deprenyl in human synovial membrane preparations from patients showing varying grades of joint inflammation: (●) grade 0 - no inflammation (n=7); (■) grade 1 - mild (n=9); (○) grade 2 - moderate (n=10); (♦) grade 3 - severe (n=4). Results were expressed as means ± SEM and analyzed with one-way analysis of variance followed by Dunnett's post-hoc test. Statistical significance was depicted as ** $p<0.01$.

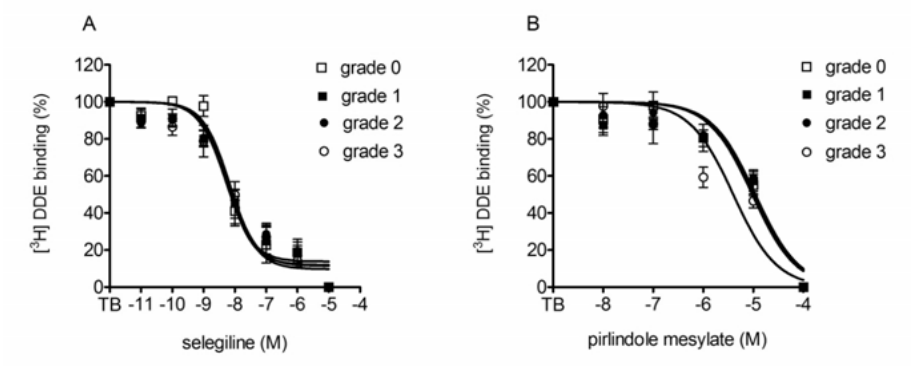

Figure 3. Competitive binding curves of selegiline (A) and pirlindole mesylate (B) in human synovial membrane preparations with varying levels of inflammation: (●) grade 0 - no inflammation (n=6); (■) grade 1 - mild (n=5); (○) grade 2 - moderate (n=9); (♦) grade 3 - severe (n=4). Synovial homogenates (200 µg/tube) were incubated for 4 h at 25°C with 10 nM [^{3}H]-D-deprenyl) and increasing concentrations of pirlindole mesylate (10^{-5} - 10^{-8} M) and selegiline (10^{-6} - 10^{-11} M). Results are expressed as means ± SEM and fitted with non-linear regression/one site sigmoidal dose-response model. There were no statistically significant differences between groups.

Biochemical characteristics of the [^{3}H]-D-deprenyl binding

Trypsin significantly reduced [^{3}H]-D-deprenyl binding by 38.6% and this effect was abolished by the addition of aprotinin (a competitive serine protease inhibitor). High temperatures (95°C), a protein denaturing agent (urea) and disruption of the lipid membranes (triton X-100) almost completely inhibited [^{3}H]-D-deprenyl binding. A metal chelator (EDTA) had no effect on binding (Figure 4).

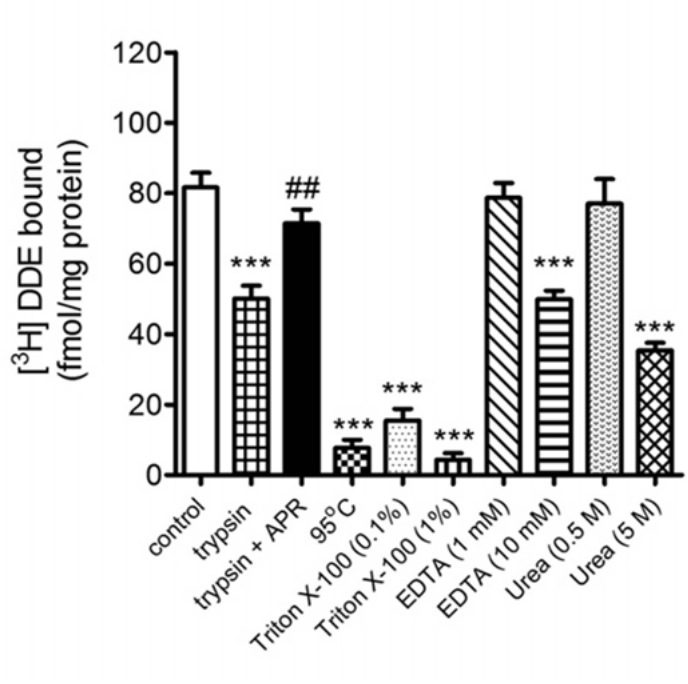

Figure 4. The effect of different treatments on [^{3}H]-D-deprenyl ([^{3}H]DDE) binding. Synovial membranes (inflammation grade: 2; 200 µg/tube) were incubated with 10 nM [^{3}H]-D-deprenyl for 4 h at 25oC in binding buffer containing trypsin (3 mg/ml), trypsin + aprotinin (0.4 mg/ml), Triton X-100, EDTA and urea. High-temperature treated samples were incubated without any additional reagents. Non-specific binding was determined with 10 µM of unlabeled D-deprenyl. Results were expressed as means ± SEM of specifically bound [^{3}H]-D-deprenyl. Statistical significance was depicted as follows: *** $p<0.001$; **$p<0.01$ (vs. control); ## $p<0.01$ (vs. trypsin).

Results from Paper III

PET/CT and [^{11}C]-D-deprenyl uptake in patients with ankle sprain

At acute phase an elevated regional [^{11}C]-D-deprenyl uptake was observed in the injured foot in all patients, with only a very low tracer uptake present in the non-injured foot. The regions of elevated tracer uptake corresponded with clinical findings and painful locations (Figure 5).

The SUV_{RATIO} showed that the regional [^{11}C]-D-deprenyl uptake in the injured locations was initially 10.7 (2.9-37.3) times higher than in the non-injured foot. [^{11}C]-D-deprenyl uptake decreased by 48% (p=0.017) between the acute investigation and first follow-up and by 50% (p=0.012) between the first and second follow-up (Figure 5). A typical case is presented in Figures 6 and 7. At later stages, additional regions of elevated [^{11}C]-D-deprenyl uptake were observed in the injured foot and even in the non-injured foot (Figure 8).

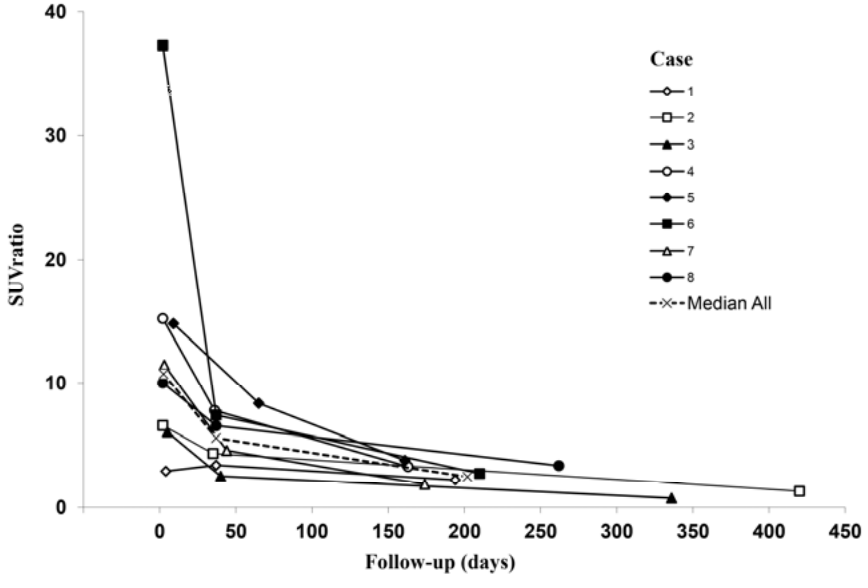

Figure 5. Median of the SUVratios (ratio of the average standardized uptake value (SUV) in the lesion to average SUV in the control region) for the eight cases. An acutely enhanced [^{11}C]-D-deprenyl uptake was significantly reduced at the first and second follow-up.

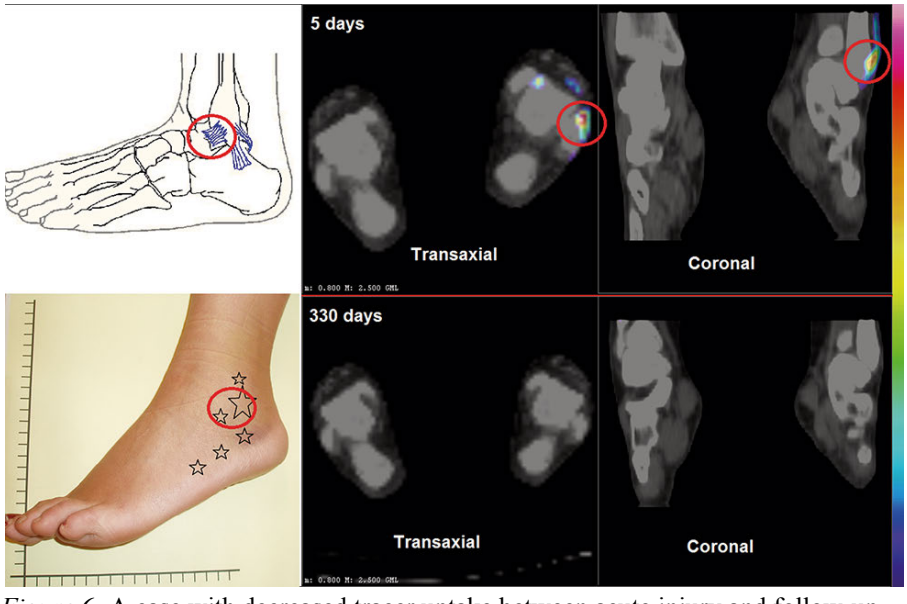

Figure 6. A case with decreased tracer uptake between acute injury and follow-up. An anatomical image and a photograph with tender points (stars) 5 days after initial injury to the left foot of a 28-year-old female (case 3) with a classic lateral inversion ankle sprain. Location of the anterior fibulotalar ligament (FTA) is indicated by a red circle in the transaxial and coronal fused [^{11}C]-D-deprenyl PET-CT images. The region of FTA initially (5 days) showed significant tracer uptake that was visually undetectable 11 months (330 days) after the injury when the patient experienced no pain at rest

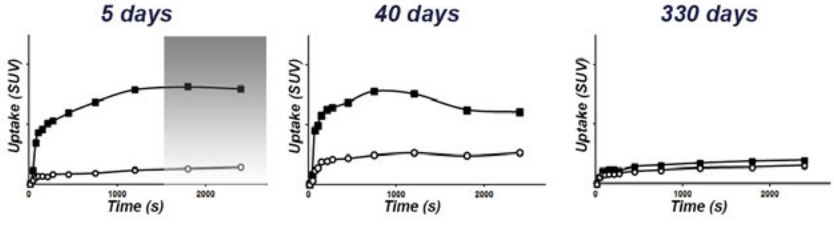

Figure 7. Respective time activity (TACT) curves from the same case as in Figure 6.

The gray rectangle indicates the data (25-45 min post-tracer administration) that were used for the generation of SUV-related parameters. The [^{11}C]-D-deprenyl uptake was undetectable 11 months after the injury indicating recovery of the tissue damage. Black rectangles represent injured the FTA and white circles the control region.

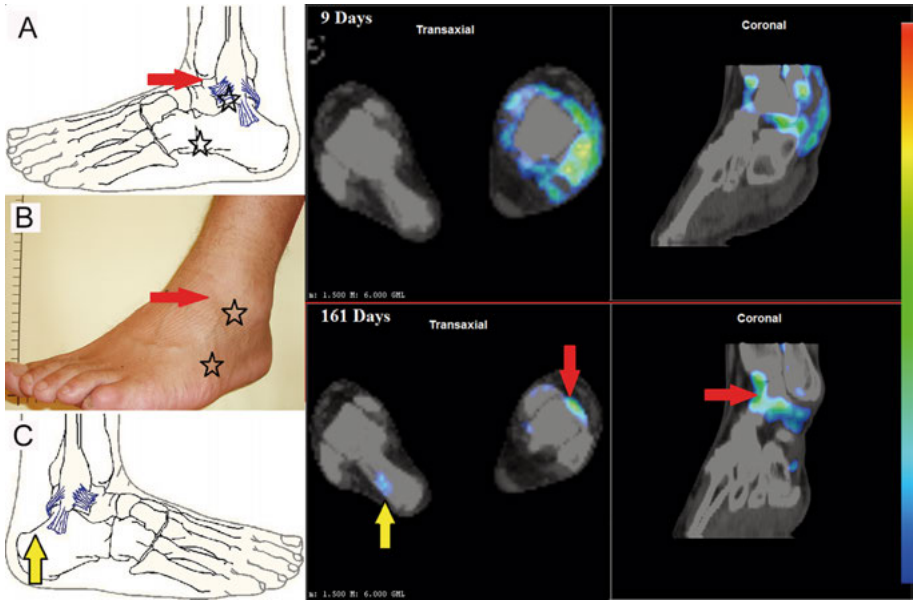

Figure 8. A case with additional regions of elevated tracer uptake. (A) An anatomical image and (B) a photograph of the left foot with tenderness points in the second follow-up 161 days after injury. The patient was a 20-year-old male (case 5) who still had a VAS score 4 at rest at the last follow-up. The tender points (stars) correspond to the anterior talofibular ligament and the calcaneocuboid joint. The red arrow represents the location of the anterior part of the ankle joint capsule where an increased and partly new [^{11}C]-D-deprenyl uptake is seen (161 days compared with 9 days). In the same fused PET-CT image, a new region of [^{11}C]-D-deprenyl uptake is present on the right non-injured foot (yellow arrow). (C) The location of this new regional tracer uptake is shown in an anatomical image of the right foot

Pain and [^{11}C]-D-deprenyl uptake

There was a correlation between the SUVratio at the second investigation and the VAS pain score at the last investigation (p=0.03). However, no other significant correlations between self-reported pain intensity at rest (VAS) and SUV values were detected. However, dichotomized pain was significantly associated with elevated [^{11}C]-D-deprenyl uptake (p=0.036). The estimated odds ratio (OR) for presence of pain for feet with elevated uptake compared with feet with no elevated uptake was OR=5.06 (Table 1).

Table 1. Pain and elevated [^{11}C]-D-deprenyl uptake

	Elevated uptake[a]	No elevated uptake	Total (%)
Pain[b]	26 (54%)	3 (6)	29 (60)
No pain	12 (25)	7 (15)	19 (40)
Total (%)	38 (79)	10 (21)	48 (100)

[a] $SUV_{MAX} > 1.2$ and/or $SUV_{RATIO} > 2.0$
[b] pain while weight bearing or in extreme motions (yes/no)

Results from paper IV

PET/CT and [^{11}C]-D-deprenyl uptake in whiplash patients

Increased [^{11}C]-D-deprenyl uptake was visually and quantitatively observed in multiple locations in upper neck regions in patients as compared with healthy controls (Figure 9). SUV_{RATIOS} >2 SD of the mean of healthy controls were observed in 22/32 (81%) of patients´ scans with a median SUVratio of 2.0 (IQR 1.7-3.0) at acute scans and 2.0 (IQR 1.7-2.4) at follow-up. During the acute investigations, an abnormal [^{11}C]-D-deprenyl uptake (SUV_{RATIO}) was observed in the muscle, bone structure, facet joint, occipital condyle, groove for spinal nerve and temporomandibular joint in 10/16 (63%), 12/16 (75%), 10/16 (63%), 5/16 (31%), 4/16 (25%) and 3/16 (19%) patients, respectively. At follow-up, abnormal [^{11}C]-D-deprenyl uptake (SUV_{RATIO}) was observed in the muscle, bone structure, facet joint, occipital condyle, groove for spinal nerve and temporomandibular joint in 6/16 (38%), 6/16 (38%), 7/16 (44 %), 5/16 (31%), 2/16 (13%) and in 2/16 (13%) patients, respectively. No statistical differences were found between the [^{11}C]-D-deprenyl uptake in acute and follow-up scans. The areas of elevated uptake in the upper neck were colocalized to painful locations and maximum tenderness points (Figure 9). The dynamics of the PET evaluations was characterized by a rapid initial increase in the first few frames, followed by a more gradual increase, generally plateauing in the last frames (Figure 9).

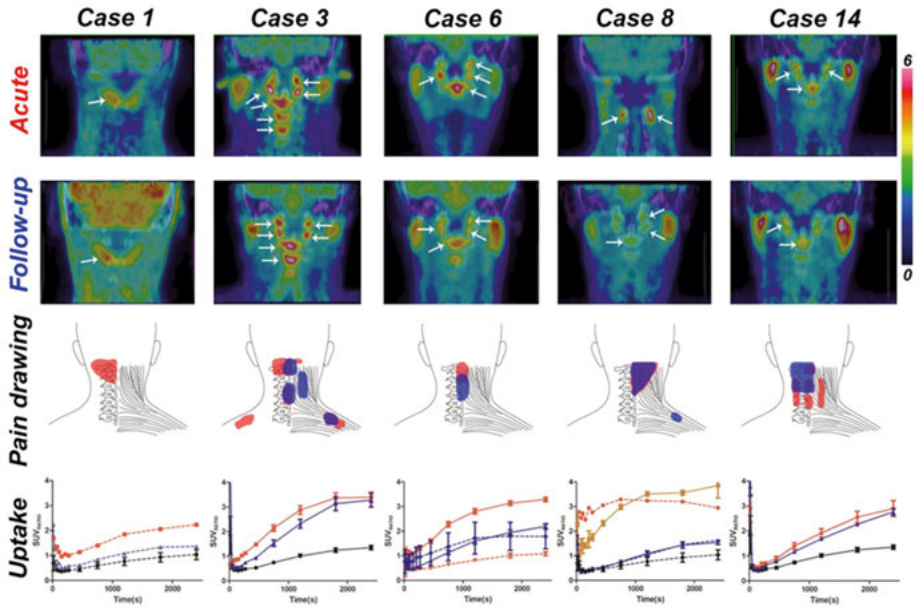

Figure 9. Comparison of five representative cases. The two top rows (***Acute and Follow-up***) represent fused transaxial [^{11}C]-D-deprenyl PET/CT images of five whiplash patients at two imaging sessions. The color bar indicates SUV_{MAX} values from 0 (dark blue) to 6 (red). These regions were colocalized to tenderness/pain locations (***Pain drawing***). The bottom row (***Uptake***) displays respective time activity curves (SUV_{RATIO} mean ± standard error). Dashed lines represent muscles and solid lines bone structures or joints. Red color indicates acute investigation, blue color follow-up and black color corresponding anatomical regions in control patients.

Pain and [^{11}C]-D-deprenyl uptake

The number of anatomical regions with an abnormal uptake was significantly and positively associated with VAS ratings (Spearman´s rank correlation 0.45, p=0.009) and NDI (Spearman´s rank correlation 0.39, p=0.028). Pairwise associations as measured by Spearman's rank correlation between uptake at different points and outcomes (VAS, CROM and NDI) revealed multiple associations between uptake (SUV_{RATIO}) in upper bone structures and facet joints for both NDI and VAS but not CROM (Figure 10). However, after taking the number of tests performed into account, no clear evidence remained between the [^{11}C]-D-deprenyl signal intensity and numerical values of the VAS, CROM or NDI.

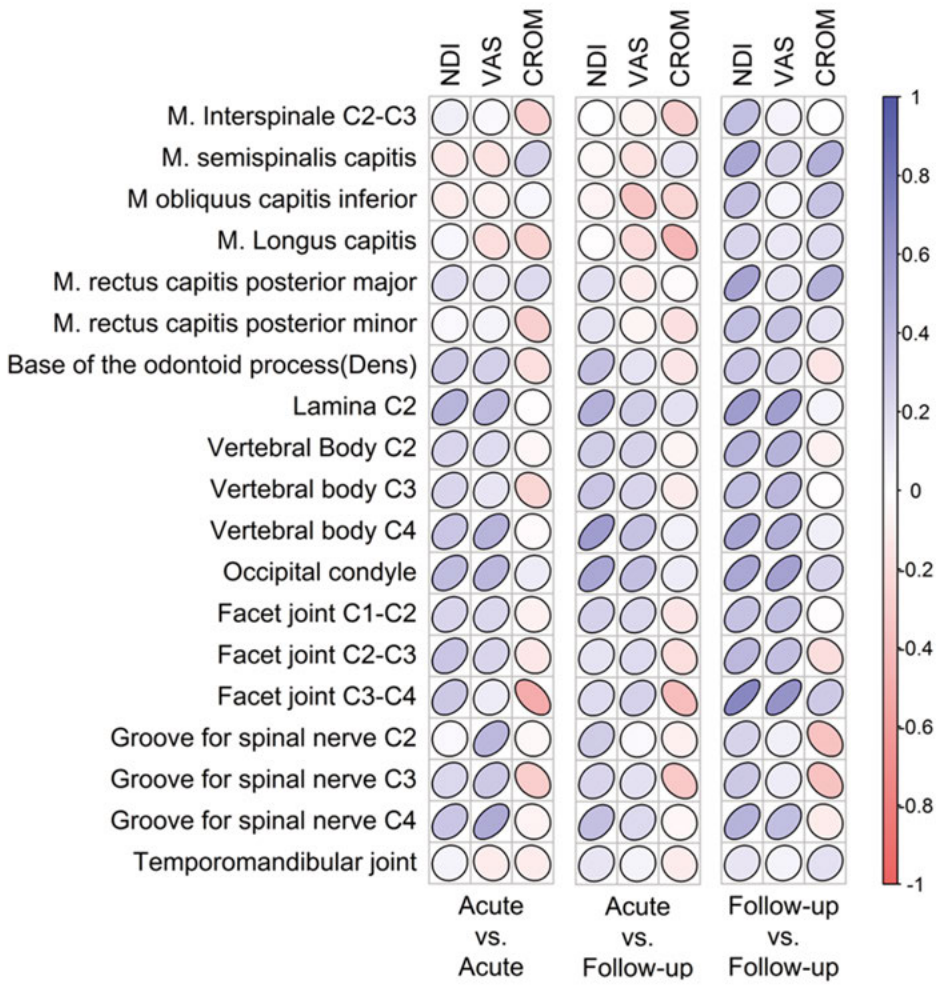

Figure 10. Anatomical regions with uptake >2 standard deviations compared with controls. Spearman rank correlation coefficients between uptake (SUV_{RATIO}) and measured outcomes. Blue represents a positive correlation and red a negative correlation. Color intensity and ellipse shape are proportional to the absolute coefficient size. For example, a symmetrical white circle represents a zero correlation coefficient while a tight blue ellipse tilted to the right mirrors a positive correlation and red to the left a negative correlation. NDI - neck disability index, VAS - visual analogue scale and CROM-cervical range of motion.

Results from Paper V

[^{11}C]-D-deprenyl

The four who underwent surgery with the model of musculoskeletal injury showed no visual uptake of the [^{11}C]-D-deprenyl. In the dynamic series, the tracer did not show accumulation in the treated leg compared with the untreated leg ($p = 0.55$).

Six rats were studied using [^{11}C]-D-deprenyl and PET in the rat model of inflammatory pain. The tracer accumulated rapidly into the inflamed ankle joint, reaching a maximum value of 1% of injected dose within 2 min (Figure 11). Lower activity was found in the untreated ankle joint, and the maximum was reached later ($p=0.001$). The ratio between ID% treated and untreated was therefore higher in the early minutes with an initial quotient of about 5, stabilizing at slightly more than 2 after 10 min.

[^{11}C]-L- dideuteriumdeprenyl

Two of the rats investigated using [^{11}C]-D-deprenyl were also studied with [^{11}C]-L-deprenyl approximately 3 hours after completion of the [^{11}C]D-deprenyl scan. Similar to [^{11}C]-D-deprenyl the tracer accumulated rapidly into the inflamed ankle joint, reaching a maximum value of 1% of injected dose within 2 min (Figure 11). Lower activity was found in the untreated ankle joint and the maximum was reached later ($p=0.001$). The ratio between ID% in treated and untreated ankle joint was higher in the early minutes, with an initial quotient of approximately 5, stabilizing at about 2 after 10 min. The time course of the uptake in the dynamic series was almost identical with [^{11}C]-D-deprenyl.

[^{18}F]fluorodeoxyglucose ([^{18}F]FDG*)*

Four rats were investigated with [^{18}F]FDG in PET. Similar to the two deprenyl tracers, [^{18}F]FDG accumulated rapidly into the inflamed ankle joint, although the maximum value was lower, approximately 0.5% of injected dose from a couple of minutes and throughout the 60 min (Figure 11). The uptake in the untreated ankle joint was markedly lower, resulting in a much higher ratio (mostly over 10) between ID% in treated and untreated ankle joint.

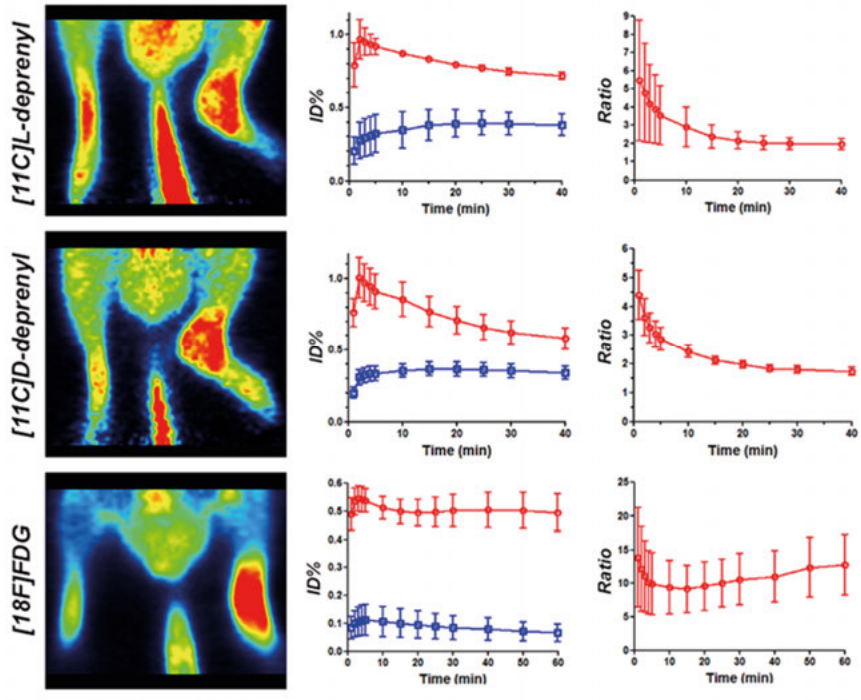

Figure 11. [^{11}C]-D-deprenyl, [^{11}C]-L-deprenyl and [^{18}F]-fluorodeoxyglucose ([18F]FDG) PET images and corresponding time activity curves of arthritic and contralateral ankles. The image in the *left column* depicts a representative image at the level of the hind limbs. The level with the highest density of uptake in each ankle joint is shown. The graph in the *middle column* is a corresponding mean time activity curve of uptake in each ankle joint expressed as percent (± sem) of injected dose (red treated, blue untreated). The curve in the *right column* displays the mean (± sem) ratio of ID% data between the treated and untreated rat ankle joint.

Discussion

Papers I and II

The possible binding targets of D-deprenyl

The established molecular target of L-deprenyl (selegiline) is MAO-B. Increased uptake of L-deprenyl indicates concomitant inflammation in the brain serving principally as an *in vivo* marker for astrocytosis[113-116]. D-deprenyl was originally used as a MAO-B inactive control in neuroimaging studies[78]. Consequently, little is known about its binding targets especially in the periphery. Previous studies suggest an increased trapping and specific binding in inflammatory pain conditions[72]. In our studies we demonstrated that D-deprenyl visualizes inflammation and that the most rational mechanism of D-deprenyl uptake is binding to MAO.

In the broad high-throughput search for binding targets for D-deprenyl, MAO enzymes (MAO-A and MAO-B) emerged as anticipated. Surprisingly, the competitive binding studies pointed out only MAO-B as a main target in that principally only L-deprenyl competed for the same site as D-deprenyl. This event was demonstrated by a specific MAO-A inhibitor (pirlindole mesylate) that displaced D-deprenyl binding with a 1000-times lower affinity compared with MAO-B selective L-deprenyl. The hypothesis describing MAO-B as the primary target for D-deprenyl stands in contrast to studies on mostly rat mitochondria [68,71], where D-deprenyl was more potent in inhibiting the MAO-A activity but also exhibited lower selectivity.

Our findings from the study on inflamed human synovia demonstrated that D-deprenyl targeted a specific saturable population of membrane-bound binding sites. The high binding affinity was in nanomolar range and appeared to involve only one target, presumably MAO-B. Little is known about role of MAO-B in peripheral inflammation or pain-generating processes. However, the idea of MAO-B being the main molecular target and a possible indicator of peripheral inflammation is plausible finds some support in the literature. One early study proposed that an overexpression of MAO-B in the synovial fluid could serve as a biomarker for the progression of rheumatoid arthritis[117]. Mature adipocytes have been shown to express high levels of MAO-B[118] and BAT with a high concentration of mitochondria has been proposed to be a possible site for D-deprenyl accumulation in whiplash patients[97]. Importantly, a substance that binds to MAO enzymes that is embedded in the outer mitochondrial membrane can also be a marker for the density of mitochondria and their activity. The parenchymal cells of the submandibular and parotid glands unaffected by inflammatory processes also exhibit high D-deprenyl retention that was further linked to increased MAO-B activity[97,119,120]. Other tracers designed to quantify the inflammatory response in arthritis also target

activated macrophages by binding to an outer mitochondrial membrane translocator protein (TSPO) and show a similar binding profile kinetics to D-deprenyl with an uptake sensitive to the level of inflammation[121-123].

The HTS enzyme assay also discovered that 70% of ACE activity (MAO-A 55%!) was inhibited by D-deprenyl in rabbit lung preparations. However, no competition for the D-deprenyl binding site was observed from an ACE inhibitor in the radioligand binding assays. ACE is an essential enzyme in bradykinin metabolism and some evidence exists on the role of ACE in inflammation [124 125,126]. Thus, there is a still slender possibility of ACE being a putative target for D-deprenyl.

We did not identify any obvious high-affinity target candidates among GPCRs. However, a weak antagonistic activity did emerge at two histamine receptor subtypes - HRH1 and HRH3. And again, the binding studies could not confirm this, expect to show a low-affinity competition of the HRH1 agonist. Thus, it is unlikely that histamine receptors are putative targets for D-deprenyl.

The binding characteristics of D-deprenyl

D-deprenyl binding was significantly reduced following incubation with a proteolytic enzyme trypsin, but restored upon addition of aprotinin (a trypsin inhibitor), our experiments describing primary biochemical properties of the binding site revealed characteristics common for proteins. Moreover, high temperature completely abolished binding, whereas an almost 60% reduction was observed upon incubation with urea. This finding indicates that denaturing agents by weakening the hydrophobic interactions within the binding target promote unfolding of the tertiary complex typical for proteins[127]. Additionally, indicating that the target is a membrane-bound protein (as mitochondrial MAO enzymes are), the integrity of the lipid bilayer was found to be essential for D-deprenyl binding as non-denaturing detergents abolish it completely[128].

We showed that D-deprenyl bound to a specific, saturable population of binding sites in a manner proportional to protein concentration and incubation time. Binding affinity was in the high nanomolar range and appeared to involve only one target. These features of D-deprenyl make it a potentially useful PET tracer[129]. Radioactively labelled D-deprenyl binding in the human inflamed synovium adopted a similar hyperbolic shape as time activity curves obtained with dynamic PET imaging in patients affected by chronic WAD[130] or as in Papers III and IV. Similarly, a rapid increase in tracer uptake in the first frames was observed until the plateau phase, proposing a specific trapping of D-deprenyl at a saturable binding site.

Surprisingly, and contrary to L-deprenyl, the labeled D-deprenyl enabled the discrimination between low- and high-grade inflammation synovitis. D-

deprenyl showed increased affinity while there were no alterations in the binding site density (~700 fmol/mg in all samples which can be compared with ~3000 in rat brain mitochondrial fraction). This unique observation strengthens further the idea of D-deprenyl being a useful peripheral inflammation marker in PET imaging studies. A possible explanation for this interesting phenomena is inflammation-induced allosteric modification of the target protein[131-133].

Strengths and limitations

The explanation for D-deprenyl´s high retention in peripheral inflammation and identification of the binding site has not been extensively investigated. Synovial membrane preparations harvested from arthritic patients offered a unique opportunity to analyze *ex vivo* kinetics of D-deprenyl binding in humans. We have shown that D-deprenyl may differentiate between a low and an elevated level of inflammation and that the most rational mechanism of D-deprenyl uptake is binding to MAO. From the literature we know that MAO has an important function in regulating the delicate balance of neurotransmitters, other biogenic amines and ROS. On the other hand, these substances are capable of modulating pain processing and generation.

It is possible that having two sample populations may contribute to different levels of inflammation and that the osteoarthritis in terms of synovial cell activation and hyperplasia is considered milder compared with rheumatoid arthritis. However, the expression of synovitis and the histological and macroscopic changes are very similar and are not so much disease-specific, which was verified by the very similar D-deprenyl binding patterns in terms of Kd and B_{max} in our study. In comparison with studies on human tissue, the competitive binding studies in rat brain mitochondrial fraction (mitochondria from CNS) comes with two main limitations. First, the direct translation of results from rat brain MAO-B to human MAO-B is difficult. This is because even though the MAO-B enzymes in these two species are highly homologous, there are 3-D structural differences that affect the enzymes' substrate specificity and sensitivities to a given inhibitor[134]. Another problem is that the proportions of MAO enzymes are different in different species and tissues. For example, in human brain MAO-B is clearly more abundant than MAO-A with a ratio of MAO-B to MAO-A varying between 2.6-17.8[135]. Another problem with studying purified proteins/receptors is that normally the recombinant technique is used only to produce the extracellular chains of the proteins and not the cytosolic nor transmembrane parts thus affecting the protein folding (chaperones), binding and possible allosteric modulations. The HTS we used in this study utilized recombinant human MAO expressed in Hi5 insect cells.

Papers III and IV

Localization of elevated [^{11}C]-D-deprenyl uptake in patients with musculoskeletal injuries

Inflammation is a common and complex response to any peripheral tissue injury, and it may cause acute and chronic pain [136,137]. In present studies we provide evidense that tissue injury and inflammation can be objectively visualized and quantified using [^{11}C]-D-deprenyl PET/CT. Accumulation of D-deprenyl tracked the normal recovery process and possible inflammation after acute traumatic musculoskeletal injury. The ratio of uptake (SUV_{RATIO}) between the injured and the reference region provided the best demonstration of high initial [^{11}C]-D-deprenyl uptake and a recovery-associated decrease.

The localization of the tracer uptake correlated with the expected anatomical localizations as the tracer uptake was localized to bones, joints and ligaments and surrounding structures and was concurrent with the clinical examinations and the mechanism of injury. The recovery process was reflected by serial PET imaging. D-deprenyl uptake appeared to take place mostly during the inflammatory phase of injury repair but was still noticeable in the proliferative and remodeling phases. The tracer uptake was evident months after the initial injury which follows the time needed for completion of healing and recovery of ankle sprains[138-140] and whiplash injury where it has been estimated that only around 50% of all patients make full recovery[45,141,142]. In both studies we found new regions of increased tracer uptake that might be the result of abnormal kinematics with ligament insufficiency and the first signs of degenerative and adaptive changes[143]. Ligament instability and impaired position sense alters the contact mechanics in the joints and muscles and causes wear and increased shear loading along with inflammatory processes [144-146]. For example, increased loading and overuse of the non-injured foot, with increased stress to the joints and bone surfaces, might cause the observed elevation in tracer uptake on the non-injured foot. Indeed, one patient, a professional dancer, described how he now "had to dance on one (the non-injured) foot" after ankle sprain injury.

Especially the findings after whiplash injury, where the uptake localized to facet joints and cervical bone structures showed positive associations with pain, are interesting because commonly used imgaing technologies cannot usually detect these lesions. This is one of the first studies to show *in vivo* the high incidense of possible peripheral structural alterations after whiplash injury. The knowledge of these injuries has been collected mostly from cadaveric, post-mortem and animal studies and not from patients[147,148].

Pain and elevated [^{11}C]-D-deprenyl uptake

There may be a relationship between [^{11}C]-D-deprenyl uptake and subsequent risk of persisting pain following trauma as the tracer uptake was positively correlated with subjective pain ratings at last follow in the ankle sprain study. This may be reasonable if the initial [^{11}C]-D-deprenyl uptake is associated with severity of injury[149]. There were no other direct correlations between subjective pain intensity and [^{11}C]-D-deprenyl uptake which is understandable because the perception of pain is not a simple linear phenomenon, and the nociceptive input can be modulated at several levels of the pain pathway, which would attenuate the direct influence of pain-generating processes at the injury site. However, pain and disability after ankle sprain coexisted with increased [^{11}C]-D-deprenyl uptake. In the whiplash study we found positive associations between [^{11}C]-D-deprenyl uptake in injured structures in the upper neck and self-reported pain and self-rated disability. This supports the lesion-based model of whiplash where the peripheral lesion are proposed to underlie the occurrence of pain and disability[150]. Interestingly, in our study on whiplash patients the subjective ratings were not positively associated with uptake in muscles in acute investigation, but at follow-up investigation there were emerging association of muscle uptake with self-rated disability (NDI) and neck mobility (CROM). This can be explained by disuse of the muscles and intramuscular "fatty infiltration" [151,152]. Because of the limits of spatial resolution in PET/CT, anatomical muscle locations may have included surrounding tissue like adipose tissue that has been proposed to be behind D-deprenyl uptake[130].

Strengths and limitations

We used a novel approach to verify and extend previous [^{11}C]-D-deprenyl PET/CT-PET findings by investigating tracer retention in unilateral isolated ankle sprain, where the intact ankle can be used as a within-subject non-affected control. The limitations of both studies were the small sample size and that the exact mechanism of D-deprenyl in inflammation is not known despite the results from Papers I and II. The small sample size gave us less statistical power to detect differences. However, we believe that the sample size was appropriate for expensive (>30 000 SEK/session) PET pilot studies to describe and assess feasibility of using [^{11}C]-D-deprenyl PET/CT. Unfortunately, we cannot provide a clear explanation of the uptake mechanism of [^{11}C]-D-deprenyl. even though binding assays suggest that MAO is the primary target of interest. Trapping mechanisms, other than binding to a specific molecular structure, are possible at the site of injury or inflammation. As the D-deprenyl molecule is a weak lipophilic base, non-specific trapping mechanisms could include elevaed blood flow, increased vascular permeability and enhanced transudation at the injury site. Sampling from an artery and full tracer kinetic

modeling had been necessary to fully exclude blood flow components of tracer uptake. To minimize but not totally eliminate the effects of blood flow, a semi-quantitative measurement of the radioactivity concentration in tissue with a reference region (SUV_{RATIO}) was used in whiplash study[153], and in both studies the analysis was done 25-45 min post-tracer administration.

In the dynamic PET, the rapid increase in the first frames was followed by a slight washout or plateau being present in the last frames, suggesting a mechanism of irreversible or slowly reversible tracer trapping. The shape of TACT curves indicates that enhanced blood flow is unlikely the sole mechanism of tracer uptake and probably as with other lipophilic tracers the uptake is a combination of an unspecific accumulation to the injury site and a specific binding. Actually, an increased blood flow and neovascularization observed with ultrasound in the upper painful neck tissues has already been described as an objective finding after whiplash injury[154].

Paper V

D-deprenyl uptake in rat models of pain

All studied ligands were able to visualize the inflamed ankle but there were no apparent differences between the uptake of the two deprenyl isomers. Much to our surprise, because D-deprenyl should be much less potent MAO-B inhibitor. We demonstrated that ^{11}C-labeled L-deprenyl and D-deprenyl accumulated in the 'unknown' binding site with identical binding curves in a rat model of inflammatory pain. These preliminary findings can be interpreted that the binding is not MAO-B dependent because D-deprenyl is considered as 25-500 times less potent as a MAO-B inhibitor[68,71]. Further, you can speculate that the uptake of [^{11}C]-D-deprenyl was related not related only to perfusion and tissue edema but also to the intensity of the inflammation. As described in a previous study[155] the low-intensity inflammation or activation of the recovery process in the rat model of postoperative pain did not show [^{11}C]-D-deprenyl uptake or any differences between treated and untreated leg. Therefore, one can assume that [^{11}C]-D-deprenyl does not show pure nociception, but more likely, the sensibility to nociception.

Furthermore, compared to the [^{18}F]FDG, the dynamic [^{11}C]-D-deprenyl PET data did not show any obvious signs of irreversible trapping or specific binding in the inflamed rat ankle. The are many possible explanations for the mechanism of this unspecific deprenyl accumulation: Elevated blood flow and metabolism, changed vascular permeability with enhanced transudation, changes in the local chemical milieu and influx of activated blood cells.

Strengths and limitations

We presented a novel way of studying and comparing PET tracers "in vivo" in an experimental animal model where untreated limb was used as a within-subject non-affected control. The used model showed to be suitable of studying a non-specific inflammation PET marker [^{18}F]FDG, but not deprenyl isomers. The findings of deprenyl uptake can be blurred by differences in species and tissues. This difference in substrate/ligand selectivity and expression of MAO-enzymes between species make it difficult to draw definitive conclusion from animal to human studies. The relative expression and proportions of each MAO isoform varies enormously across different tissues, species and even cells[156]. There are functional and structural properties that differentiate human MAO-A and rat MAO-A [157,158] and for example human MAO-A exhibits a 10-fold lower affinity than rat MAO-A for the specific inhibitor clorgyline[159]. Furthermore, rat and human MAO B are highly homologous, but there are 3-D structural differences that affect the substrate specificity and sensitivities of the enzymes to a given inhibitor[134]. There is also a possibility that injury and inflammation can upregulate the expression of MAO-isomers in different ways and that the ligand affinity to these enzymes changes[62,63,160]. It must be remembered that in *in vivo* studies MAO can also be brought to the site of tissue injury by the migrating leukocytes or other cells from the blood. Even though it appears that human and rat MAO profiles are quite similar compared to many other species[161], histological studies would have been needed to confirm the presence and expression of different MAO isoforms in the inflamed rat ankle. The spatial resolution of PET bring also limitations in determinating the exact localization of tracer uptake in a small inflamed rat ankle. The ROIs may include different types of tissues (the tissue fraction effect) and tissue edema with possible tracer dilution can have caused an underestimation of the tracer uptake.

Clinical implications and future research

There is accumulating evidence that pain, wound healing and inflammation are closely linked. Moreover, acute inflammation is an essential consequence of almost any tissue injury, and both inflammatory cells and inflammatory mediators play a significant role in pain generation. It is therefore of immence importance to find means of selectively visualizing inflamed tissue. It would help to find a diagnosis, a suitable treatment and to follow the treatment response in the individual patient. If we can see inflammation, we also can visualize a pain-generating process corresponding to the sites where the patient reports pain and that there is a pathophysiological reason for pain experience. 'Pain generators' are not any more invisible. PET/CT with a suitable specific

tracer can bring a possible tool for studying chronic musculoskeletal pain where other methods have seldom pointed out any peripheral findings.

Our data showing that it is possible to find an objective marker of peripheral pain-generating processes and inflammation in pain patients are important for pain diagnostics and to confirm the patients self-report. It may also provide us with a better understanding of the peripheral mechanism, pathophysiology and localization of pain in individual patients and even chronic pain syndromes. We still do not know how acute pain from a peripheral injury becomes chronic pain. Our findings and methods can contribute to a better understanding of the importance of peripheral and central mechanism to the total experience of pain and add to the methods used for the diagnostics work-up for chronic pain patients. PET imaging is the study of function and activity at a molecular level and not merely anatomical structure. PET can therefore be used to not only differentiate between tissues with normal and abnormal function but it can also facilitate the implication of 'precision medicine'. In particular, the association between the D-deprenyl uptake in the cervical bone structures and facet joints and the development of persistent pain and disability contributes to a better understanding of affected peripheral structures and mechanisms behind WAD.

Irradiation is a problem with PET but theoretically finding a ^{11}C-tracer will reduce the radioactive dose to three-fold compared with a ^{18}F-tracer (FDG) that is now commonly used for imaging inflammation.

Further studies are still needed to elucidate the exact uptake mechanism of D-deprenyl and to characterize what parts of the injury-inflammation cascade are visualized by [^{11}C]-D-Deprenyl PET. Prospective cohort studies with a sufficient sample size and follow-up are needed to further elucidate the predictive and diagnostic value peripheral D-deprenyl PET in chronic pain syndromes. A more rigorous pain analysis and a measurement of disability are needed in future studies to address the link between peripheral pain induction on the molecular level and subjective pain experience. Future studies are also warranted to make direct head-to-head comparisons between different techniques (PET/MRI) and other possible tracers. Because a high site-specificity is required, it may be the MAO-B specific D-deprenyl enantiomer [^{11}C]-L-deprenyl and specific radiolabeled MAO-A ligands that deserve further exploration regarding sensitivity and specificity in human pain and inflammatory pain syndromes instead of animal models.

Conclusions from my thesis:

The high-throughput analysis indicates the existence of three enzyme targets for D-deprenyl: MAO-A, MAO-B and ACE. Subsequent radioligand receptor binding assays in rat mitochondrial and whole cell brain fractions point to MAO-B as the major target.

The binding site in human inflamed synovia appears to be a membrane-bound protein that may be distinct from MAO-B, even though MAO-B has a vital role in D-deprenyl retention.

D-deprenyl differentiates between low and high grades of inflammation which makes it a potentially useful tracer in imaging of inflammation.

[^{11}C]-D-deprenyl PET can be used to visualize, quantify and follow inflammation and pain-generating processes in peripheral tissue.

[^{11}C]-D-deprenyl PET may be valuable to identify patients with problematic healing and prolonged inflammation and who are at elevated risk of developing persistent pain.

Organic lesions in upper cervical bone structures and facet joints that are detectable with PET/CT may be relevant for the development of persistent pain and disability in whiplash injury.

The experimental rat models of inflammation and surgical pain may not be useful for the development and evaluation of MAO PET tracers.

Populärvetenskaplig sammanfattning (Summary in Swedish)

Smärta är mycket vanligt och man räknar att ca 20 % av befolkningen lider av långvarig smärta i någon grad. Smärta är också en unik personlig upplevelse och därför är patientens egna skattningar av smärtintensiteten och subjektiva beskrivning av smärtan fortfarande den ”gyllene normen”. Smärta är därför på många vis ”en osynlig sjukdom”. Eftersom objektiva fynd ofta saknas vid många typer av smärttillstånd, finns en risk att patienten inte blir riktigt förstådd av behandlare i sjukvården - ”man hittar inger fel”. Ett objektivt och opartiskt sätt att avbilda, påvisa och mäta processer som ger upphov till smärtan i perifer vävnad skulle innebära ett framsteg i smärtforskningen. En radioaktiv markör, [11C]-D-deprenyl, har i tidigare studier visat ett förhöjt upptag i inflammerad och smärtande vävnad, men den exakta upptagsmekanismen har varit okänd.

För att närmare studera bindningsmekanismen för D-deprenyl, undersökte vi bindningen till 250 olika enzymer och proteiner och kunde visa att D-deprenyl binder starkast till ett enzym som finns i mitokondrierna och kallas för monoaminoxidas-B (MAO-B) som har viktiga biologiska och medicinska funktioner. Fortsatta studier på inflammerade ledhinnor från patienter visade att D-deprenyl binder till ett protein som sitter inbäddat i cellmembran, och att D-deprenyl-bindningen kan skilja mellan olika grader av inflammation. Allt detta talar för att D-deprenyl skulle kunna fungera som en lämplig inflammationsmarkör inom smärtforskningen.

Trots att perifer inflammation och vävnadsskada är en viktig orsak till smärtupplevelsen finns det ytters få studier där man har försökt lokalisera och mäta graden av inflammation i en vävnadsskada. Med en medicinsk avbildningsteknik, positronemissons-tomografi (PET), som bygger på användning av radioaktiva markörer, går det att skapa bilder av kroppens struktur och funktion. Vi gjorde en PET studie på patienter med ensidig fotledsstukning och kunde visa att alla patienter hade ett tydligt förhöjd [11C]-D-deprenyl upptag kring det stukade smärtsamma ledbandet, och inget upptag i den friska foten. Studien visade också att upptaget kunde mätas, och kvarstående upptag stämde väl överens med patientens upplevelse av smärta. Det här tyder på att D-deprenyl PET kan användas för avbildning av inflammation i perifer vävnadsskada och kan vara en objektiv markör för perifera smärtprocesser.

Efter en kraftig översträckning av mjukdelarna och skeletten i nacken (så kallad pisksnärtskada eller whiplash-skada) kan det uppstå långvariga problem med smärta, huvudvärk och stelhet i nackmusklerna. Whiplashskador svarar för en stor del personskador och långvariga hälsoförluster efter bilolyckor i västvärlden. Orsaken till smärtan och obehaget är dock oklar, och det har varit svårt att objektivt diagnostisera eller avbilda någon vävnadsskada

med vanlig röntgen eller magnetkamera. I denna avhandlingens huvudstudie undersökte vi whiplash – drabbade patienter direkt efter inträffad trafikolycka och efter 6 månader och kunde se att inflammation och vävnadsskadan kan avbildas med hjälp av D-deprenyl PET. Som i studien med stukade fötter kunde vi följa upp och objektivt mäta upptaget av D-deprenyl i skadade nackområden. Vi kunde också visa att D-deprenyl togs upp i nackens skelettstrukturer och leder och hade ett samband med smärtskattningar och upplevd funktionsnedsättning. Detta talar för att perifer D-deprenyl PET – undersökning kan användas för diagnostik och uppföljning hos kroniska smärtpatienter med denna typ av skada.

För att ytterligare studera mekanismen bakom D-deprenyl upptag i skadad och smärtande vävnad, jämförde vi D-deprenyl med sin ”spegelbild” L-deprenyl, och ett av det vanligaste spårämnena vid inflammation [^{18}F]FDG, i två olika råttmodeller; en modell för inflammation och en för kirurgiskt inducerat trauma. Överraskande och i motsats till våra förväntningar sågs ackumuleringen av D-deprenyl bara i den inflammatoriska smärtmodellen. Denne var identiskt med L-deprenyl upptaget och visade inga tecken på specifik bindning eller att spårämnet fångades upp i cellerna. En förklaring kan vara att skillnaderna mellan MAO enzymerna hos råtta och människa är allt för stora. Detta talar för att deprenyl inte bör studeras vidare i de djurmodeller vi använt.

Acknowledgements

This thesis would not have been possible without the help and commitment of a vast number of people. Therefore, I would like to express my sincere gratitude to:

Torsten Gordh, my principal supervisor, for engaging me in and always being enthusiastic and confident about this project, for his patience, guidance, understanding, respect and all challenging work and financial support, and for employing me as a young anaesthesiology resident.

Jens Sörensen, my co-supervisor, for stimulating discussions, for sharing your knowledge in your field, and for always being patient with beginner´s questions despite an immense personal workload. Your time with me has been very much appreciated.

Magnus Peterson, my second co-supervisor, for helpful discussions and for teaching me how to become a good supervisor.

Mats Fredrikson and Clas Linnman, for advice, as well as for your invaluable support concerning the conception, design, execution and interpretation of the human studies.

Anna Lesniak, for making the preclinical studies possible and for all your expertise. Without you this thesis would be far less than what it is now.

The people of Uppsala Berzelii Technology Centre of Neurodiagnostics, especially **Thomas Norberg** and **Fred Nyberg** for your support and profound knowledge in your respective fields.

The staff of Uppsala University PET Centre, especially **Gunnar Antoni**, **Mark Lubbering**, **Lieuwe Appel** and **Lars Lindsjö**, for helping to interpret and retrieve data.

The staff of Uppsala University Preclinical PET Platform, especially **Håkan Hall** for all his excellent help and expertise.

Sten Rubertsson, for providing an excellent environment for my doctoral studies, even though I did not do my thesis in an intensive care setting.

The past-and-present heads of the Department of Anesthesiology and Critical Care at Akademiska Sjukhuset, **Göran Angergård**, **Johann Valtysson**, **Suzanne Odeberg Werneman** and the heads of the Critical Care Department

Rafael Kawati and **Lucian Covaciu**, for making it possible to combine clinical practice with research and at the same time encourage and support me to drive my dissertation to completion.

Katja Andersson, **Siv Andersson** and **Elin Eriksson** provided invaluable assistance in connection with my doctoral studies.

My loving mother **Maija** for putting me through school, believing in me and being there, and my father **Kari**, for being such a good father the past years, and my mother-in-law **Maisa,** for all her support with the family.

My children: **Lukas, Ines and Ellen**, for giving my life a purpose and making me feel happy.

My wife **Riina**, for loving and living by my side throughout my adult life and supporting me in every possible way.

References

1. Bonica JJ. The need of a taxonomy. *Pain.* 1979;6(3):247-248.
2. Smith SM, Hunsinger M, McKeown A, et al. Quality of Pain Intensity Assessment Reporting: ACTTION Systematic Review and Recommendations. *J Pain.* 2015;16(4):299-305.
3. Marchand S. *The Phenomenon of PAIN.* IASP press; 2012.
4. Basbaum AI, Bautista DM, Scherrer G, Julius D. Cellular and molecular mechanisms of pain. *Cell.* 2009;139(2):267-284.
5. Schmidt R, Schmelz M, Forster C, Ringkamp M, Torebjörk E, Handwerker H. Novel classes of responsive and unresponsive C nociceptors in human skin. *J Neurosci.* 1995;15(1 Pt 1):333-341.
6. Apkarian AV, Bushnell MC, Treede RD, Zubieta JK. Human brain mechanisms of pain perception and regulation in health and disease. *Eur J Pain.* 2005;9(4):463-484.
7. Caterina MJ, Schumacher MA, Tominaga M, Rosen TA, Levine JD, Julius D. The capsaicin receptor: a heat-activated ion channel in the pain pathway. *Nature.* 1997;389(6653):816-824.
8. Fernandes ES, Fernandes MA, Keeble JE. The functions of TRPA1 and TRPV1: moving away from sensory nerves. *Br J Pharmacol.* 2012;166(2):510-521.
9. Tominaga M, Caterina MJ, Malmberg AB, et al. The cloned capsaicin receptor integrates multiple pain-producing stimuli. *Neuron.* 1998;21(3):531-543.
10. Bautista DM, Jordt SE, Nikai T, et al. TRPA1 mediates the inflammatory actions of environmental irritants and proalgesic agents. *Cell.* 2006;124(6):1269-1282.
11. Nassar MA, Stirling LC, Forlani G, et al. Nociceptor-specific gene deletion reveals a major role for Nav1.7 (PN1) in acute and inflammatory pain. *Proc Natl Acad Sci U S A.* 2004;101(34):12706-12711.
12. Bohlen CJ, Chesler AT, Sharif-Naeini R, et al. A heteromeric Texas coral snake toxin targets acid-sensing ion channels to produce pain. *Nature.* 2011;479(7373):410-414.
13. Chuang HH, Prescott ED, Kong H, et al. Bradykinin and nerve growth factor release the capsaicin receptor from PtdIns(4,5)P2-mediated inhibition. *Nature.* 2001;411(6840):957-962.
14. Ji RR, Chamessian A, Zhang YQ. Pain regulation by non-neuronal cells and inflammation. *Science.* 2016;354(6312):572-577.

15. Studenic P, Radner H, Smolen JS, Aletaha D. Discrepancies between patients and physicians in their perceptions of rheumatoid arthritis disease activity. *Arthritis Rheum.* 2012;64(9):2814-2823.
16. Sharma NK, Ryals JM, Liu H, Liu W, Wright DE. Acidic saline-induced primary and secondary mechanical hyperalgesia in mice. *J Pain.* 2009;10(12):1231-1241.
17. Deval E, Lingueglia E. Acid-Sensing Ion Channels and nociception in the peripheral and central nervous systems. *Neuropharmacology.* 2015;94:49-57.
18. Baron A, Lingueglia E. Pharmacology of acid-sensing ion channels - Physiological and therapeutical perspectives. *Neuropharmacology.* 2015;94:19-35.
19. Gregory NS, Brito RG, Fusaro MC, Sluka KA. ASIC3 Is Required for Development of Fatigue-Induced Hyperalgesia. *Mol Neurobiol.* 2016;53(2):1020-1030.
20. Kessler W, Kirchhoff C, Reeh PW, Handwerker HO. Excitation of cutaneous afferent nerve endings in vitro by a combination of inflammatory mediators and conditioning effect of substance P. *Exp Brain Res.* 1992;91(3):467-476.
21. HARDY JD, WOLFF HG, GOODELL H. Experimental evidence on the nature of cutaneous hyperalgesia. *J Clin Invest.* 1950;29(1):115-140.
22. Perl ER, Kumazawa T, Lynn B, Kenins P. Sensitization of high threshold receptors with unmyelinated (C) afferent fibers. *Prog Brain Res.* 1976;43:263-277.
23. Woolf CJ. Evidence for a central component of post-injury pain hypersensitivity. *Nature.* 1983;306(5944):686-688.
24. Melzack R, Wall PD. Pain mechanisms: a new theory. *Science.* 1965;150(3699):971-979.
25. Moore KA, Kohno T, Karchewski LA, Scholz J, Baba H, Woolf CJ. Partial peripheral nerve injury promotes a selective loss of GABAergic inhibition in the superficial dorsal horn of the spinal cord. *J Neurosci.* 2002;22(15):6724-6731.
26. Chen GY, Nuñez G. Sterile inflammation: sensing and reacting to damage. *Nat Rev Immunol.* 2010;10(12):826-837.
27. Rock KL, Latz E, Ontiveros F, Kono H. The sterile inflammatory response. *Annu Rev Immunol.* 2010;28:321-342.
28. Fullerton JN, Gilroy DW. Resolution of inflammation: a new therapeutic frontier. *Nat Rev Drug Discov.* 2016;15(8):551-567.
29. Zelenka M, Schäfers M, Sommer C. Intraneural injection of interleukin-1beta and tumor necrosis factor-alpha into rat sciatic nerve at physiological doses induces signs of neuropathic pain. *Pain.* 2005;116(3):257-263.
30. Ren K, Torres R. Role of interleukin-1beta during pain and inflammation. *Brain Res Rev.* 2009;60(1):57-64.

31. Lieberthal J, Sambamurthy N, Scanzello CR. Inflammation in joint injury and post-traumatic osteoarthritis. *Osteoarthritis Cartilage.* 2015;23(11):1825-1834.
32. Moradi B, Rosshirt N, Tripel E, et al. Unicompartmental and bicompartmental knee osteoarthritis show different patterns of mononuclear cell infiltration and cytokine release in the affected joints. *Clin Exp Immunol.* 2015;180(1):143-154.
33. Scanzello CR. Chemokines and inflammation in osteoarthritis: Insights from patients and animal models. *J Orthop Res.* 2016.
34. Ramesh G. Novel Therapeutic Targets in Neuroinflammation and Neuropathic Pain. *Inflamm Cell Signal.* 2014;1(3).
35. Lord JM, Midwinter MJ, Chen YF, et al. The systemic immune response to trauma: an overview of pathophysiology and treatment. *Lancet.* 2014;384(9952):1455-1465.
36. Li J, Chen J, Kirsner R. Pathophysiology of acute wound healing. *Clin Dermatol.* 2007;25(1):9-18.
37. Smith C, Kruger MJ, Smith RM, Myburgh KH. The inflammatory response to skeletal muscle injury: illuminating complexities. *Sports Med.* 2008;38(11):947-969.
38. Shin EH, Caterson EJ, Jackson WM, Nesti LJ. Quality of healing: defining, quantifying, and enhancing skeletal muscle healing. *Wound Repair Regen.* 2014;22 Suppl 1:18-24.
39. Müller SA, Todorov A, Heisterbach PE, Martin I, Majewski M. Tendon healing: an overview of physiology, biology, and pathology of tendon healing and systematic review of state of the art in tendon bioengineering. *Knee Surg Sports Traumatol Arthrosc.* 2015;23(7):2097-2105.
40. Kim MH, Liu W, Borjesson DL, et al. Dynamics of neutrophil infiltration during cutaneous wound healing and infection using fluorescence imaging. *J Invest Dermatol.* 2008;128(7):1812-1820.
41. Martin P, Leibovich SJ. Inflammatory cells during wound repair: the good, the bad and the ugly. *Trends Cell Biol.* 2005;15(11):599-607.
42. Davis CG. Mechanisms of chronic pain from whiplash injury. *J Forensic Leg Med.* 2013;20(2):74-85.
43. Spitzer WO, Skovron ML, Salmi LR, et al. Scientific monograph of the Quebec Task Force on Whiplash-Associated Disorders: redefining "whiplash" and its management. *Spine (Phila Pa 1976).* 1995;20(8 Suppl):1S-73S.
44. Sterner Y, Gerdle B. Acute and chronic whiplash disorders--a review. *J Rehabil Med.* 2004;36(5):193-209; quiz 210.
45. Chappuis G, Soltermann B, CEA, AREDOC, CEREDOC. Number and cost of claims linked to minor cervical trauma in Europe: results from the comparative study by CEA, AREDOC and CEREDOC. *Eur Spine J.* 2008;17(10):1350-1357.

46. Lord SM, Barnsley L, Wallis BJ, Bogduk N. Chronic cervical zygapophysial joint pain after whiplash. A placebo-controlled prevalence study. *Spine (Phila Pa 1976).* 1996;21(15):1737-1744; discussion 1744-1735.
47. Styrke J, Stålnacke BM, Bylund PO, Sojka P, Björnstig U. A 10-year incidence of acute whiplash injuries after road traffic crashes in a defined population in northern Sweden. *PM R.* 2012;4(10):739-747.
48. Whiplashkommissionen. *The Whiplash Commission Final Report.* 2005.
49. Anderson SE, Boesch C, Zimmermann H, et al. Are there cervical spine findings at MR imaging that are specific to acute symptomatic whiplash injury? A prospective controlled study with four experienced blinded readers. *Radiology.* 2012;262(2):567-575.
50. Matsumoto M, Okada E, Ichihara D, et al. Prospective ten-year follow-up study comparing patients with whiplash-associated disorders and asymptomatic subjects using magnetic resonance imaging. *Spine (Phila Pa 1976).* 2010;35(18):1684-1690.
51. Holm LW, Carroll LJ, Cassidy JD, et al. The burden and determinants of neck pain in whiplash-associated disorders after traffic collisions: results of the Bone and Joint Decade 2000-2010 Task Force on Neck Pain and Its Associated Disorders. *J Manipulative Physiol Ther.* 2009;32(2 Suppl):S61-69.
52. Kamper SJ, Rebbeck TJ, Maher CG, McAuley JH, Sterling M. Course and prognostic factors of whiplash: a systematic review and meta-analysis. *Pain.* 2008;138(3):617-629.
53. Stovner LJ. The nosologic status of the whiplash syndrome: a critical review based on a methodological approach. *Spine (Phila Pa 1976).* 1996;21(23):2735-2746.
54. Ferrari R. *The Whipalsh Encyclopedia: The Facts and Myths about Whiplash.* Jones and BArtlett publishers; 2005.
55. Berry MD, Juorio AV, Paterson IA. The functional role of monoamine oxidases A and B in the mammalian central nervous system. *Prog Neurobiol.* 1994;42(3):375-391.
56. Kitahama K, Maeda T, Denney RM, Jouvet M. Monoamine oxidase: distribution in the cat brain studied by enzyme- and immunohistochemistry: recent progress. *Prog Neurobiol.* 1994;42(1):53-78.
57. Donnelly CH, Murphy DL. Substrate- and inhibitor-related characteristics of human platelet monoamine oxidase. *Biochem Pharmacol.* 1977;26(9):853-858.
58. Balsa MD, Gómez N, Unzeta M. Characterization of monoamine oxidase activity present in human granulocytes and lymphocytes. *Biochim Biophys Acta.* 1989;992(2):140-144.
59. Nagakura Y, Takahashi M, Noto T, et al. Different pathophysiology underlying animal models of fibromyalgia and neuropathic pain:

comparison of reserpine-induced myalgia and chronic constriction injury rats. *Behav Brain Res.* 2012;226(1):242-249.
60. Adams JD, Odunze IN. Oxygen free radicals and Parkinson's disease. *Free Radic Biol Med.* 1991;10(2):161-169.
61. Wittmann C, Chockley P, Singh SK, Pase L, Lieschke GJ, Grabher C. Hydrogen peroxide in inflammation: messenger, guide, and assassin. *Adv Hematol.* 2012;2012:541471.
62. Chaitidis P, Billett EE, O'Donnell VB, et al. Th2 response of human peripheral monocytes involves isoform-specific induction of monoamine oxidase-A. *J Immunol.* 2004;173(8):4821-4827.
63. Cathcart MK, Bhattacharjee A. Monoamine oxidase A (MAO-A): a signature marker of alternatively activated monocytes/macrophages. *Inflamm Cell Signal.* 2014;1(4).
64. Gupta V, Khan AA, Sasi BK, Mahapatra NR. Molecular mechanism of monoamine oxidase A gene regulation under inflammation and ischemia-like conditions: key roles of the transcription factors GATA2, Sp1 and TBP. *J Neurochem.* 2015;134(1):21-38.
65. Manoli I, Le H, Alesci S, et al. Monoamine oxidase-A is a major target gene for glucocorticoids in human skeletal muscle cells. *FASEB J.* 2005;19(10):1359-1361.
66. Lam CS, Li JJ, Tipoe GL, Youdim MBH, Fung ML. Monoamine oxidase A upregulated by chronic intermittent hypoxia activates indoleamine 2,3-dioxygenase and neurodegeneration. *PLoS One.* 2017;12(6):e0177940.
67. Salter-Cid LM, Wang E, O'Rourke AM, et al. Anti-inflammatory effects of inhibiting the amine oxidase activity of semicarbazide-sensitive amine oxidase. *J Pharmacol Exp Ther.* 2005;315(2):553-562.
68. Magyar K, Vizi E, Ecseri Z, Knoll J. Comparative pharmacological analysis of the optical isomers of phenyl-isopropyl-methyl-propinylamine (E-250). *Acta Physiol Acad Sci Hung.* 1967;32(4):377-387.
69. Knoll J, Ecseri Z, Kelemen K, Nievel J, Knoll B. Phenylisopropylmethylpropinylamine (E-250), a new spectrum psychic energizer. *Arch Int Pharmacodyn Ther.* 1965;155(1):154-164.
70. Knoll J, Magyar K. Some puzzling pharmacological effects of monoamine oxidase inhibitors. *Adv Biochem Psychopharmacol.* 1972;5:393-408.
71. Robinson JB. Stereoselectivity and isoenzyme selectivity of monoamine oxidase inhibitors. Enantiomers of amphetamine, N-methylamphetamine and deprenyl. *Biochem Pharmacol.* 1985;34(23):4105-4108.
72. Danfors T, Bergström M, Feltelius N, Ahlström H, Westerberg G, Långström B. Positron emission tomography with 11C-D-deprenyl in

patients with rheumatoid arthritis. Evaluation of knee joint inflammation before and after intra-articular glucocorticoid treatment. *Scand J Rheumatol.* 1997;26(1):43-48.
73. Maruyama W, Naoi M. Neuroprotection by (-)-deprenyl and related compounds. *Mech Ageing Dev.* 1999;111(2-3):189-200.
74. Thiffault C, Quirion R, Poirier J. The effect of L-deprenyl, D-deprenyl and MDL72974 on mitochondrial respiration: a possible mechanism leading to an adaptive increase in superoxide dismutase activity. *Brain Res Mol Brain Res.* 1997;49(1-2):127-136.
75. Muralikrishnan D, Samantaray S, Mohanakumar KP. D-deprenyl protects nigrostriatal neurons against 1-methyl-4-phenyl-1,2,3,6-tetrahydropyridine-induced dopaminergic neurotoxicity. *Synapse.* 2003;50(1):7-13.
76. Fang J, Yu P. Effect of L-deprenyl, its structural analogues and some monoamine oxidase inhibitors on dopamine uptake. *Neuropharmacology.* 1994;33(6):763-768.
77. Tábi T, Magyar K, Szöko E. Chiral characterization of deprenyl-N-oxide and other deprenyl metabolites by capillary electrophoresis using a dual cyclodextrin system in rat urine. *Electrophoresis.* 2003;24(15):2665-2673.
78. Fowler JS, MacGregor RR, Wolf AP, et al. Mapping human brain monoamine oxidase A and B with 11C-labeled suicide inactivators and PET. *Science.* 1987;235(4787):481-485.
79. Fowler JS, Logan J, Shumay E, Alia-Klein N, Wang GJ, Volkow ND. Monoamine oxidase: radiotracer chemistry and human studies. *J Labelled Comp Radiopharm.* 2015;58(3):51-64.
80. McBride HM, Neuspiel M, Wasiak S. Mitochondria: more than just a powerhouse. *Curr Biol.* 2006;16(14):R551-560.
81. Nunnari J, Suomalainen A. Mitochondria: in sickness and in health. *Cell.* 2012;148(6):1145-1159.
82. Giles RE, Blanc H, Cann HM, Wallace DC. Maternal inheritance of human mitochondrial DNA. *Proc Natl Acad Sci U S A.* 1980;77(11):6715-6719.
83. Fox TD. Mitochondrial protein synthesis, import, and assembly. *Genetics.* 2012;192(4):1203-1234.
84. Reiter RJ, Tan DX, Rosales-Corral S, Galano A, Zhou XJ, Xu B. Mitochondria: Central Organelles for Melatonin's Antioxidant and Anti-Aging Actions. *Molecules.* 2018;23(2).
85. Vafai SB, Mootha VK. Mitochondrial disorders as windows into an ancient organelle. *Nature.* 2012;491(7424):374-383.
86. Detmer SA, Chan DC. Functions and dysfunctions of mitochondrial dynamics. *Nat Rev Mol Cell Biol.* 2007;8(11):870-879.
87. Chandel NS. Mitochondria as signaling organelles. *BMC Biol.* 2014;12:34.

88. Lehnig AC, Stanford KI. Exercise-induced adaptations to white and brown adipose tissue. *J Exp Biol.* 2018;221(Pt Suppl 1).
89. Tran TT, Kahn CR. Transplantation of adipose tissue and stem cells: role in metabolism and disease. *Nat Rev Endocrinol.* 2010;6(4):195-213.
90. Bargut TC, Aguila MB, Mandarim-de-Lacerda CA. Brown adipose tissue: Updates in cellular and molecular biology. *Tissue Cell.* 2016;48(5):452-460.
91. Nedergaard J, Bengtsson T, Cannon B. Unexpected evidence for active brown adipose tissue in adult humans. *Am J Physiol Endocrinol Metab.* 2007;293(2):E444-452.
92. Cypess AM, Lehman S, Williams G, et al. Identification and importance of brown adipose tissue in adult humans. *N Engl J Med.* 2009;360(15):1509-1517.
93. Zingaretti MC, Crosta F, Vitali A, et al. The presence of UCP1 demonstrates that metabolically active adipose tissue in the neck of adult humans truly represents brown adipose tissue. *FASEB J.* 2009;23(9):3113-3120.
94. Kajimura S, Saito M. A new era in brown adipose tissue biology: molecular control of brown fat development and energy homeostasis. *Annu Rev Physiol.* 2014;76:225-249.
95. Hany TF, Gharehpapagh E, Kamel EM, Buck A, Himms-Hagen J, von Schulthess GK. Brown adipose tissue: a factor to consider in symmetrical tracer uptake in the neck and upper chest region. *Eur J Nucl Med Mol Imaging.* 2002;29(10):1393-1398.
96. Yeung HW, Grewal RK, Gonen M, Schöder H, Larson SM. Patterns of (18)F-FDG uptake in adipose tissue and muscle: a potential source of false-positives for PET. *J Nucl Med.* 2003;44(11):1789-1796.
97. Linnman C, Appel L, Fredrikson M, et al. Elevated [11C]-D-deprenyl uptake in chronic Whiplash Associated Disorder suggests persistent musculoskeletal inflammation. *PLoS One.* 2011;6(4):e19182.
98. Basu S, Zhuang H, Torigian D, Rosenbaum J, Chen W, Alavi A. Functional imaging of inflammatory diseases using nuclear medicine techniques. *Semin Nucl Med.* 2009;39(2):124-145.
99. Gotthardt M, Bleeker-Rovers CP, Boerman OC, Oyen WJ. Imaging of inflammation by PET, conventional scintigraphy, and other imaging techniques. *J Nucl Med.* 2010;51(12):1937-1949.
100. Vaidyanathan S, Patel CN, Scarsbrook AF, Chowdhury FU. FDG PET/CT in infection and inflammation--current and emerging clinical applications. *Clin Radiol.* 2015;70(7):787-800.
101. Wu C, Li F, Niu G, Chen X. PET imaging of inflammation biomarkers. *Theranostics.* 2013;3(7):448-466.
102. Moses WW. Fundamental Limits of Spatial Resolution in PET. *Nucl Instrum Methods Phys Res A.* 2011;648 Supplement 1:S236-S240.

103. Townsend DW. Combined positron emission tomography-computed tomography: the historical perspective. *Semin Ultrasound CT MR.* 2008;29(4):232-235.
104. Pollard TD. A guide to simple and informative binding assays. *Mol Biol Cell.* 2010;21(23):4061-4067.
105. Hulme EC, Trevethick MA. Ligand binding assays at equilibrium: validation and interpretation. *Br J Pharmacol.* 2010;161(6):1219-1237.
106. Youdas JW, Garrett TR, Suman VJ, Bogard CL, Hallman HO, Carey JR. Normal range of motion of the cervical spine: an initial goniometric study. *Phys Ther.* 1992;72(11):770-780.
107. Vernon H, Mior S. The Neck Disability Index: a study of reliability and validity. *J Manipulative Physiol Ther.* 1991;14(7):409-415.
108. Thie J. Understanding the standardized uptake value, its methods, and implications for usage. *J Nucl Med.* 2004;45(9):1431-1434.
109. Butler SH, Godefroy F, Besson JM, Weil-Fugazza J. A limited arthritic model for chronic pain studies in the rat. *Pain.* 1992;48(1):73-81.
110. Kiss I, Degryse AD, Bardin L, Gomez de Segura IA, Colpaert FC. The novel analgesic, F 13640, produces intra- and postoperative analgesia in a rat model of surgical pain. *Eur J Pharmacol.* 2005;523(1-3):29-39.
111. Agresti, Alan. *Foundations of Linear and Generalized Linear Models.* Wiley; 2015.
112. Westfall PH, Young SS. On adjusting P-values for multiplicity1993:941-945, Biometrics.
113. Marutle A, Gillberg PG, Bergfors A, et al. ^{3}H-deprenyl and ^{3}H-PIB autoradiography show different laminar distributions of astroglia and fibrillar β-amyloid in Alzheimer brain. *J Neuroinflammation.* 2013;10:90.
114. Schöll M, Carter SF, Westman E, et al. Early astrocytosis in autosomal dominant Alzheimer's disease measured in vivo by multi-tracer positron emission tomography. *Sci Rep.* 2015;5:16404.
115. Johansson A, Engler H, Blomquist G, et al. Evidence for astrocytosis in ALS demonstrated by [11C](L)-deprenyl-D2 PET. *J Neurol Sci.* 2007;255(1-2):17-22.
116. Santillo AF, Gambini JP, Lannfelt L, et al. In vivo imaging of astrocytosis in Alzheimer's disease: an ^{11}C-L-deuteriodeprenyl and PIB PET study. *Eur J Nucl Med Mol Imaging.* 2011;38(12):2202-2208.
117. Igari T, Shimamura T. Serotonin metabolism and its enzymic activities in joint diseases. *Clin Orthop Relat Res.* 1979(139):232-249.

118. Bour S, Daviaud D, Gres S, et al. Adipogenesis-related increase of semicarbazide-sensitive amine oxidase and monoamine oxidase in human adipocytes. *Biochimie.* 2007;89(8):916-925.
119. Almgren O, Anden NE, Jonason J, Norberg KA, Olson L. Cellular localization of monoamine oxidase in rat salivary glands. *Acta Physiol Scand.* 1966;67(1):21-26.
120. Goridis C, Neff NH. Monoamine oxidase: an approximation of turnover rates. *J Neurochem.* 1971;18(9):1673-1682.
121. Kropholler MA, Boellaard R, Elzinga EH, et al. Quantification of (R)-[11C]PK11195 binding in rheumatoid arthritis. *Eur J Nucl Med Mol Imaging.* 2009;36(4):624-631.
122. Pottier G, Bernards N, Dolle F, Boisgard R. [(1)(8)F]DPA-714 as a biomarker for positron emission tomography imaging of rheumatoid arthritis in an animal model. *Arthritis Res Ther.* 2014;16(2):R69.
123. van der Laken CJ, Elzinga EH, Kropholler MA, et al. Noninvasive imaging of macrophages in rheumatoid synovitis using 11C-(R)-PK11195 and positron emission tomography. *Arthritis Rheum.* 2008;58(11):3350-3355.
124. Kang KW. Angiotensin II-mediated Nrf2 down-regulation: a potential causing factor for renal fibrosis? *Arch Pharm Res.* 2011;34(5):695-697.
125. Maicas N, Ferrandiz ML, Brines R, et al. Deficiency of Nrf2 accelerates the effector phase of arthritis and aggravates joint disease. *Antioxid Redox Signal.* 2011;15(4):889-901.
126. Wruck CJ, Fragoulis A, Gurzynski A, et al. Role of oxidative stress in rheumatoid arthritis: insights from the Nrf2-knockout mice. *Ann Rheum Dis.* 2011;70(5):844-850.
127. Zangi R, Zhou R, Berne BJ. Urea's action on hydrophobic interactions. *J Am Chem Soc.* 2009;131(4):1535-1541.
128. le Maire M, Champeil P, Moller JV. Interaction of membrane proteins and lipids with solubilizing detergents. *Biochim Biophys Acta.* 2000;1508(1-2):86-111.
129. Friden M, Wennerberg M, Antonsson M, Sandberg-Stall M, Farde L, Schou M. Identification of positron emission tomography (PET) tracer candidates by prediction of the target-bound fraction in the brain. *EJNMMI research.* 2014;4(1):50.
130. Linnman C, Appel L, Fredrikson M, et al. Elevated [11C]-D-deprenyl uptake in chronic Whiplash Associated Disorder suggests persistent musculoskeletal inflammation. *PLoS One.* 2011;6(4):e19182.
131. Gade AR, Kang M, Akbarali HI. Hydrogen sulfide as an allosteric modulator of ATP-sensitive potassium channels in colonic inflammation. *Mol Pharmacol.* 2013;83(1):294-306.
132. Jacoby DB, Gleich GJ, Fryer AD. Human eosinophil major basic protein is an endogenous allosteric antagonist at the inhibitory muscarinic M2 receptor. *J Clin Invest.* 1993;91(4):1314-1318.

133. Zollner C, Shaqura MA, Bopaiah CP, Mousa S, Stein C, Schafer M. Painful inflammation-induced increase in mu-opioid receptor binding and G-protein coupling in primary afferent neurons. *Mol Pharmacol.* 2003;64(2):202-210.
134. Novaroli L, Daina A, Favre E, et al. Impact of species-dependent differences on screening, design, and development of MAO B inhibitors. *J Med Chem.* 2006;49(21):6264-6272.
135. Tong J, Meyer JH, Furukawa Y, et al. Distribution of monoamine oxidase proteins in human brain: implications for brain imaging studies. *J Cereb Blood Flow Metab.* 2013;33(6):863-871.
136. Lee YC. Effect and treatment of chronic pain in inflammatory arthritis. *Curr Rheumatol Rep.* 2013;15(1):300.
137. Linley JE, Rose K, Ooi L, Gamper N. Understanding inflammatory pain: ion channels contributing to acute and chronic nociception. *Pflugers Arch.* 2010;459(5):657-669.
138. Hubbard T, Hicks-Little C. Ankle ligament healing after an acute ankle sprain: an evidence-based approach. *J Athl Train.* 2008;43(5):523-529.
139. Konradsen L, Bech L, Ehrenbjerg M, Nickelsen T. Seven years follow-up after ankle inversion trauma. *Scand J Med Sci Sports.* 2002;12(3):129-135.
140. van Rijn RM, van Os AG, Bernsen RM, Luijsterburg PA, Koes BW, Bierma-Zeinstra SM. What is the clinical course of acute ankle sprains? A systematic literature review. *Am J Med.* 2008;121(4):324-331.e326.
141. Gargan MF, Bannister GC. The rate of recovery following whiplash injury. *Eur Spine J.* 1994;3(3):162-164.
142. Berglund A, Bodin L, Jensen I, Wiklund A, Alfredsson L. The influence of prognostic factors on neck pain intensity, disability, anxiety and depression over a 2-year period in subjects with acute whiplash injury. *Pain.* 2006;125(3):244-256.
143. Hintermann B, Boss A, Schäfer D. Arthroscopic findings in patients with chronic ankle instability. *Am J Sports Med.* 2002;30(3):402-409.
144. Hirose K, Murakami G, Minowa T, Kura H, Yamashita T. Lateral ligament injury of the ankle and associated articular cartilage degeneration in the talocrural joint: anatomic study using elderly cadavers. *J Orthop Sci.* 2004;9(1):37-43.
145. Fleming B, Hulstyn M, Oksendahl H, Fadale P. Ligament Injury, Reconstruction and Osteoarthritis. *Curr Opin Orthop.* 2005;16(5):354-362.
146. Revel M, Andre-Deshays C, Minguet M. Cervicocephalic kinesthetic sensibility in patients with cervical pain. *Arch Phys Med Rehabil.* 1991;72(5):288-291.
147. Taylor JR, Twomey LT. Acute injuries to cervical joints. An autopsy study of neck sprain. *Spine (Phila Pa 1976).* 1993;18(9):1115-1122.

148. Panjabi MM, Ito S, Pearson AM, Ivancic PC. Injury mechanisms of the cervical intervertebral disc during simulated whiplash. *Spine (Phila Pa 1976).* 2004;29(11):1217-1225.
149. Clay FJ, Watson WL, Newstead SV, McClure RJ. A systematic review of early prognostic factors for persisting pain following acute orthopedic trauma. *Pain Res Manag.* 2012;17(1):35-44.
150. Curatolo M, Bogduk N, Ivancic PC, McLean SA, Siegmund GP, Winkelstein BA. The role of tissue damage in whiplash-associated disorders: discussion paper 1. *Spine (Phila Pa 1976).* 2011;36(25 Suppl):S309-315.
151. Elliott J, Jull G, Noteboom JT, Darnell R, Galloway G, Gibbon WW. Fatty infiltration in the cervical extensor muscles in persistent whiplash-associated disorders: a magnetic resonance imaging analysis. *Spine (Phila Pa 1976).* 2006;31(22):E847-855.
152. Elliott J, Pedler A, Kenardy J, Galloway G, Jull G, Sterling M. The temporal development of fatty infiltrates in the neck muscles following whiplash injury: an association with pain and posttraumatic stress. *PLoS One.* 2011;6(6):e21194.
153. Adams MC, Turkington TG, Wilson JM, Wong TZ. A systematic review of the factors affecting accuracy of SUV measurements. *AJR Am J Roentgenol.* 2010;195(2):310-320.
154. Hatem K, Britt-Marie S, Martin F, Lars Ö, Felix L, Håkan A. New objective findings after whiplash injury: High blood flow in painful cervical soft tissues: An ultrasound pilot study. In. Scandinavian Journal of Pain: Elsevier; 2013:173-179.
155. Tegler G, Sörensen J, Ericson K, Björck M, Wanhainen A. 4D-PET/CT with [(11)C]-PK11195 and [(11)C]-(D)-deprenyl does not identify the chronic inflammation in asymptomatic abdominal aortic aneurysms. *Eur J Vasc Endovasc Surg.* 2013;45(4):351-356.
156. Dorris RL. A simple method for screening monoamine oxidase (MAO) inhibitory drugs for type preference. *J Pharmacol Methods.* 1982;7(2):133-137.
157. Kwan SW, Abell CW. cDNA cloning and sequencing of rat monoamine oxidase A: comparison with the human and bovine enzymes. *Comp Biochem Physiol B.* 1992;102(1):143-147.
158. Chen ZY, Hotamisligil GS, Huang JK, et al. Structure of the human gene for monoamine oxidase type A. *Nucleic Acids Res.* 1991;19(16):4537-4541.
159. Tsugeno Y, Hirashiki I, Ogata F, Ito A. Regions of the molecule responsible for substrate specificity of monoamine oxidase A and B: a chimeric enzyme analysis. *J Biochem.* 1995;118(5):974-980.
160. Villeneuve C, Guilbeau-Frugier C, Sicard P, et al. p53-PGC-1α pathway mediates oxidative mitochondrial damage and cardiomyocyte necrosis induced by monoamine oxidase-A

upregulation: role in chronic left ventricular dysfunction in mice. *Antioxid Redox Signal.* 2013;18(1):5-18.

161. Inoue H, Castagnoli K, Van Der Schyf C, Mabic S, Igarashi K, Castagnoli N. Species-dependent differences in monoamine oxidase A and B-catalyzed oxidation of various C4 substituted 1-methyl-4-phenyl-1,2,3, 6-tetrahydropyridinyl derivatives. *J Pharmacol Exp Ther.* 1999;291(2):856-864.

Acta Universitatis Upsaliensis

Digital Comprehensive Summaries of Uppsala Dissertations from the Faculty of Medicine 1456

Editor: The Dean of the Faculty of Medicine

A doctoral dissertation from the Faculty of Medicine, Uppsala University, is usually a summary of a number of papers. A few copies of the complete dissertation are kept at major Swedish research libraries, while the summary alone is distributed internationally through the series Digital Comprehensive Summaries of Uppsala Dissertations from the Faculty of Medicine. (Prior to January, 2005, the series was published under the title "Comprehensive Summaries of Uppsala Dissertations from the Faculty of Medicine".)

Distribution: publications.uu.se
urn:nbn:se:uu:diva-347685

ACTA
UNIVERSITATIS
UPSALIENSIS
UPPSALA
2018